Theory of Josephson effects in anisotropic superconductors

Yukio Tanaka
Graduate School of Science and Technology and Department of Physics, Niigata University, Ikarashi, Niigata 950-21, Japan

Satoshi Kashiwaya
Electrotechnical Laboratory, Tsukuba, Ibaraki 305, Japan

(Received 2 January 1997)

An analytical formula for the dc Josephson current in anisotropic singlet superconductor/insulator/anisotropic singlet superconductor junctions is presented. The formula is applicable for junctions with arbitrary insulating-potential height and thickness and with any symmetries including d-wave superconductors. In contrast to the formulas for conventional s-wave superconductors, the formula includes two additional effects. One is the intrinsic phase of the pair potential originating from the pairing symmetry in anisotropic superconductors. The other is the formation of localized states around the insulator. Using this formula, the Josephson current is calculated in s-wave superconductor/insulator/$d_{x^2-y^2}$-wave superconductor ($s/I/d$) and $d_{x^2-y^2}$-wave superconductor/insulator/$d_{x^2-y^2}$-wave superconductor ($d/I/d$) junction configurations. In the case of the ($d/I/d$) junction, the anomalous temperature dependence of the maximum Josephson current is calculated. This behavior is completely different from that expected for s-wave superconductors. The validity of a phenomenological theory by Sigrist and Rice [J. Phys. Soc. Jpn. **61**, 4283 (1992)] is also discussed. [S0163-1829(97)06625-3]

I. INTRODUCTION

In order to reveal the origin of superconductivity in high-T_c superconductors, the symmetries of the pair potentials have been investigated under various situations for several years now. A growing amount of evidence has accumulated recently, based on various theories and experimental data,[1–7] which point to the $d_{x^2-y^2}$-wave symmetry of the pair potentials. In particular, the observation of anomalous magnetic field dependences in π junctions[8–11] clearly verified that the pair potential in high-T_c superconductors encounters a phase change between a- and b-axis directions.[11–13] Moreover, several other measurements, using superconducting quantum-interference devices (SQUID's), Josephson junctions, or tricrystal rings[14–20] showed results which are consistent with $d_{x^2-y^2}$-wave symmetry of the pair potentials. These experimental results are considered to be the most rigid evidence for d-wave symmetry because they utilize the phase sensitive nature of the Josephson junctions. On the other hand, the properties of the Josephson junctions in d-wave superconductors have not been sufficiently revealed. The above experimental results are analyzed in terms of a phenomenological theory which is a simple extension of the theory for conventional s-wave superconductors. To fully understand the experimental data, a new theory for the Josephson junctions in d-wave superconductors constructed on a microscopic basis is needed.

A trial along this direction was done by one of us (Y.T.). The dc Josephson current between an s-wave superconductor/insulator/$d_{x^2-y^2}$-wave superconductor ($s/I/d$) junction with $a(x)$, $b(y)$, and $c(z)$ axis orientation is calculated by taking into account Andreev reflection[21] and the normal reflection at the interface.[22] This theory explains the anomalous magnetic field dependence of the maximum Josephson current $I_c(T)$ of the corner junction and corner SQUID (Refs. 12 and 13) naturally. In addition to this theory, several theories of Josephson junctions containing d-wave superconductors have been presented which take into account the anisotropy of the pair potential.[23–30] Although all of them have succeeded in revealing some aspects of the Josephson effect, one more essential effect, the existence of zero-energy states (ZES's) around the insulator, has not been introduced yet.

The formation of ZES's at the surface of d_{xy}-wave superconductors was pointed out by Hu.[31] On the other hand, the existence of zero-bias conductance peaks (ZBCP's) at the surface of high-T_c superconductors has been confirmed by several tunneling spectroscopy measurements.[32–40] It has been revealed based on a tunneling theory[41–43] that the experimental ZBCP's are closely related to the ZES's at the surface of d-wave superconductors. These ZES's are induced for the reason that the pair potential in high-T_c superconductors incurs a change in sign in some region of the Fermi surface.[44–46] The theory which explains the various experimental line shapes of tunneling conductance[47–51] is completely distinct from that for an s-wave superconductor in the sense that the tunneling spectroscopy is essentially sensitive to the phase of the pair potentials.[42,43] The fundamental concept for the formation of ZES's is simple.[52] At the surface of anisotropic superconductors, a conducting quasiparticle is reflected and changes its direction. At the same time, the effective pair potential felt by the quasiparticle changes. The ZES's are formed[53–62] when the effective pair potential incurs a change in sign through the reflection. In Ref. 52, the physical origin of the ZES's in several nonuniform superconductors are discussed in a unified way based on the quantum condition of the bound states of the quasiparticles. Similar effects can also be expected in Josephson junctions including d-wave superconductors[41] as the boundary effect around the insulator. In such situations, under the influence of the exis-

tence of ZES's, the properties of the Josephson current in $s/I/d$ and $d/I/d$ junctions are expected to become anomalous[63–65] as can be inferred from the properties of $s/I/s$ junctions.[66–72]

In this paper, we present an analytical formula for the dc Josephson current which fully takes into account the bound states around the insulator as well as the anisotropy of the pair potential. Although the self-consistency of the pair potential is neglected, the formula can be applicable to arbitrary barrier height and for spin-singlet superconductors with any symmetry including d-wave and $(s+id)$-wave (time-reversed symmetry-breaking case) superconductors.[73–77] The obtained formula has a general form, and several existing theories can be derived from the formula as limiting cases.[66,69,78,79] Using the formula, the Josephson current in $d/I/d$ and $s/I/d$ junctions is analyzed in detail. The organization of this paper is as follows. In Sec. II, a model for the Josephson current is given and the formula to calculate it is explicitly derived. The physical meaning of the formula is discussed in detail. In Sec. III, we clarify basic properties of $s/I/d$ junctions. The Josephson current in the corner SQUID configurations is also discussed. In Sec. IV, we address the basic properties of $d/I/d$ junctions. We calculate the grain angle dependence of the Josephson current. The validity of the theory by Sigrist and Rice[11] (referred to as SR theory) is discussed. In Sec. V the formula is extended to a three-dimensional model. The Josephson current along the c axis is calculated. In Sec. VI, we summarize our results.

II. MODEL AND FORMULATION

The Josephson current formula used in this study is essentially the extension of the previous formula for s-wave superconductors[78–79] that includes the anisotropy of the pair potential. The formula is subsequently derived along with the original one. We start from the Bogoliubov–de Gennes (BdG) equations

$$Eu_n(\mathbf{x}_1)=h_0u_n(\mathbf{x}_1)+\int d\mathbf{x}_2\Delta(\mathbf{s},\mathbf{r})v_n(\mathbf{x}_2),$$

$$Ev_n(\mathbf{x}_1)=-h_0v_n(\mathbf{x}_1)+\int d\mathbf{x}_2\Delta^*(\mathbf{s},\mathbf{r})u_n(\mathbf{x}_2), \qquad (1)$$

with $\mathbf{s}=(\mathbf{x}_1-\mathbf{x}_2)$, $\mathbf{r}=(\mathbf{x}_1+\mathbf{x}_2)/2$, and $h_0=-\hbar^2\nabla^2_{\mathbf{x}_1}/2m+U(x)-\mu$, where μ, $U(x)$, and E are the chemical potential, the Hartree potential, and the energy of a quasiparticle measured from the Fermi energy E_F ($E_F=\mu$), respectively. The functions $u_n(\mathbf{x}_1)$ and $v_n(\mathbf{x}_1)$ are the eigenfunction of the BdG equations. The electron field operators $\Psi_\sigma(\mathbf{x}_1,t)$ ($\sigma=\uparrow$ or $\downarrow$) satisfy the equation

$$i\hbar\frac{\partial}{\partial t}\Psi_\uparrow(\mathbf{x}_1,t)=h_0\Psi_\uparrow(\mathbf{x}_1,t)+\int d\mathbf{x}_2\Delta(\mathbf{s},\mathbf{r})\Psi^\dagger_\downarrow(\mathbf{x}_2,t), \qquad (2)$$

$$i\hbar\frac{\partial}{\partial t}\Psi^\dagger_\downarrow(\mathbf{x}_1,t)=-h_0\Psi^\dagger_\downarrow(\mathbf{x}_1,t)+\int d\mathbf{x}_2\Delta^*(\mathbf{s},\mathbf{r})\Psi_\uparrow(\mathbf{x}_2,t). \qquad (3)$$

The field operators are expanded using the eigenfunctions of BdG equations as

$$\Psi_\uparrow(\mathbf{x}_1,t)=\sum_n[\alpha_{n,\uparrow}u_n(\mathbf{x}_1)\exp(-iE_nt/\hbar)-\alpha^\dagger_{n,\downarrow}v^*_n(\mathbf{x}_1)\exp(iE_nt/\hbar)], \qquad (4)$$

$$\Psi^\dagger_\downarrow(\mathbf{x}_1,t)=\sum_n[\alpha_{n,\uparrow}v_n(\mathbf{x}_1)\exp(-iE_nt/\hbar)+\alpha^\dagger_{n,\downarrow}u^*_n(\mathbf{x}_1)\exp(iE_nt/\hbar)], \qquad (5)$$

where the summation is taken over all the eigenstates with positive energies E_n and $\alpha_{n,\sigma}$ ($\alpha^\dagger_{n,\sigma}$) is the annihilation (creation) operator for a quasiparticle. According to the method of Blonder, Tinkham, and Klapwijk,[80] we can define the electric charge density P_e ($e>0$), the electric current $\mathbf{J}_e$, and the source term S as

$$P_e=-e[\Psi^\dagger_\uparrow(\mathbf{x},t)\Psi_\uparrow(\mathbf{x},t)+\Psi^\dagger_\downarrow(\mathbf{x},t)\Psi_\downarrow(\mathbf{x},t)], \qquad (6)$$

$$\mathbf{J}_e=-\frac{e\hbar}{m}\,\mathrm{Im}[\Psi^\dagger_\uparrow(\mathbf{x},t)\boldsymbol{\nabla}\Psi_\uparrow(\mathbf{x},t)+\Psi^\dagger_\downarrow(\mathbf{x},t)\boldsymbol{\nabla}\Psi_\downarrow(\mathbf{x},t)], \qquad (7)$$

$$S=-\frac{2e}{\hbar}\,\mathrm{Im}\left\{\int d\mathbf{x}''d\mathbf{x}'\Delta(\mathbf{x},\mathbf{x}'')[\Psi^\dagger_\uparrow(\mathbf{x}'',t)\Psi^\dagger_\downarrow(\mathbf{x}',t)+\Psi^\dagger_\uparrow(\mathbf{x}',t)\Psi^\dagger_\downarrow(\mathbf{x}'',t)]\right\}. \qquad (8)$$

These three quantities satisfy the conservation law given as

$$\frac{\partial P_e}{\partial t}+\boldsymbol{\nabla}\cdot\mathbf{J}_e=S. \qquad (9)$$

For the simplest model calculation, we consider a two-dimensional anisotropic singlet-superconductor/insulator/anisotropic singlet-superconductor junction with perfectly flat interfaces in the clean limit. The system is assumed to be in the equilibrium state. In this model, the interface is perpendicular to the x axis and is located at $x=0$ and $x=d_i$, where d_i is the magnitude of the thickness of the insulating region. The Fermi wave number k_F and the effective mass m are assumed to be equal both in the left- and the right-side superconductors. The pair potential and Hartree potential are assumed to be

$$\Delta(\mathbf{k},\mathbf{r})=\begin{cases}\overline{\Delta_L}(\gamma)\exp(i\varphi_L), & x<0,\\ 0, & 0<x<d_i,\\ \overline{\Delta_R}(\gamma)\exp(i\varphi_R), & x>d_i,\end{cases}$$

$$U(x)=\begin{cases}0, & x<0,\\ U_0, & 0<x<d_i,\\ 0, & x>d_i,\end{cases} \qquad (10)$$

where $\Delta(\mathbf{k},\mathbf{r})$ is the Fourier transform of $\Delta(\mathbf{s},\mathbf{r})$, with

$\exp(i\gamma)\equiv k_x/|\mathbf{k}|+ik_y/|\mathbf{k}|$ using a wave vector $\mathbf{k}$.[44–46] In the weak-coupling limit, $\mathbf{k}$ is fixed on the Fermi surface ($|\mathbf{k}|=k_F$). The quantities φ_L and φ_R are the macroscopic phases of the left and right superconductors, respectively. Since the translational invariance for the y direction is satisfied, $\mathbf{J}_e$ and S depend only on x. The Josephson current $I(\varphi)$, where $\varphi=\varphi_L-\varphi_R$, between the left and right superconductors is given as

$$I(\varphi)=J_{ex}+k_BT\sum_{\omega_n}\frac{2e}{\hbar}\int_0^x \mathrm{Im}\left\{\int\int \Delta(\mathbf{x}_1,\mathbf{x}')[\mathbf{G}_{12}(\mathbf{x}'',\mathbf{x}',i\omega_n)+\mathbf{G}_{12}(\mathbf{x}',\mathbf{x}'',i\omega_n)]d\mathbf{x}'d\mathbf{x}''\right\}dx_1, \tag{11}$$

$$\mathbf{G}(\mathbf{x},\mathbf{x}',i\omega_n)=\int_0^\beta \mathbf{G}(\mathbf{x},\mathbf{x}',\tau,\tau')\exp[i\omega_n(\tau-\tau')]d\tau, \tag{12}$$

$$\mathbf{G}(\mathbf{x},\mathbf{x}',\tau,\tau')=-\begin{pmatrix}\langle T_\tau\{\Psi_\uparrow(\mathbf{x},\tau)\Psi_\uparrow^\dagger(\mathbf{x}',\tau')\}\rangle & \langle T_\tau\{\Psi_\uparrow(\mathbf{x},\tau)\Psi_\downarrow(\mathbf{x}',\tau')\}\rangle\\ \langle T_\tau\{\Psi_\downarrow^\dagger(\mathbf{x},\tau)\Psi_\uparrow^\dagger(\mathbf{x}',\tau')\}\rangle & \langle T_\tau\{\Psi_\downarrow^\dagger(\mathbf{x},\tau)\Psi_\downarrow(\mathbf{x}',\tau')\}\rangle\end{pmatrix}. \tag{13}$$

Here $\mathbf{G}(\mathbf{x},\mathbf{x}',i\omega_n)$ is a two-component Matsubara Green's function. Since the translational invariance is satisfied, the momentum parallel to the interface, $k_y=k_F\sin\gamma$, is conserved. Taking this fact into account, the Green's function is transformed into a function k_y. From the conservation of the Josephson current for $E_{Fx}\gg|\overline{\Delta_L(\gamma)}|,|\overline{\Delta_R(\gamma)}|$ with $E_{Fx}=\hbar^2k_F^2\cos^2\gamma/2m$, $I(\varphi)$ is reduced as

$$I(\varphi)=\frac{e\hbar k_BT}{2im}\lim_{x'\to x}\left(\frac{\partial}{\partial x'}-\frac{\partial}{\partial x}\right)\sum_{\omega_n,k_y}\mathrm{Tr}\{\mathbf{G}(x,x',k_y,i\omega_n)\}|_{x=0}. \tag{14}$$

In the following, the Green's function is actually calculated in the junction configuration by extending the previous method.[81] In this method, we assume four types of quasiparticle injection processes from both sides of the junction as the elementary processes shown in Fig. 1 in Ref. 41. It is important to note that the quasiparticles ''feel'' different pair potentials depending on the directions of their motions in anisotropic superconductors. For a given energy $E>(\max[|\overline{\Delta_R(\gamma_+)}|,|\overline{\Delta_R(\gamma_-)}|,|\overline{\Delta_L(\gamma_+)}|,|\overline{\Delta_L(\gamma_-)}|])$, with $\gamma_+=\gamma$ and $\gamma_-=\pi-\gamma$, the wave functions $\mathbf{\Psi}_l(\mathbf{x})$ $(l=1,\ldots,4)$ corresponding to the four processes are expressed as

$$\mathbf{\Psi}_l(\mathbf{x})=\exp(ik_Fy\sin\gamma)\Psi_l(x,\gamma)\quad(l=1,\ldots,4), \tag{15}$$

$$\Psi_1(x,\gamma)=\begin{cases}\psi_{\alpha,L}(x,\gamma)+a_1\psi_{\overline{\alpha},L}(x,\gamma)+b_1\psi_{\beta,L}(x,\gamma) & (x<0),\\ \psi_{1,I}(x,\gamma), & (0<x<d_i),\\ g_1\psi_{\alpha,R}(x,\gamma)+h_1\psi_{\overline{\beta},R}(x,\gamma), & (x>d_i),\end{cases} \tag{16}$$

$$\Psi_2(x,\gamma)=\begin{cases}\psi_{\overline{\beta},L}(x,\gamma)+a_2\psi_{\beta,L}(x,\gamma)+b_2\psi_{\overline{\alpha},L}(x,\gamma), & (x<0),\\ \psi_{2,I}(x,\gamma), & (0<x<d_i),\\ g_2\psi_{\overline{\beta},R}(x,\gamma)+h_2\psi_{\alpha,R}(x,\gamma), & (x>d_i),\end{cases} \tag{17}$$

$$\Psi_3(x,\gamma)=\begin{cases}g_3\psi_{\beta,L}(x,\gamma)+h_3\psi_{\overline{\alpha},L}(x,\gamma), & (x<0),\\ \psi_{3,I}(x,\gamma), & (0<x<d_i),\\ \psi_{\beta,R}(x,\gamma)+a_3\psi_{\overline{\beta},R}(x,\gamma)+b_3\psi_{\alpha,R}(x,\gamma), & (x>d_i),\end{cases} \tag{18}$$

$$\Psi_4(x,\gamma)=\begin{cases}g_4\psi_{\overline{\alpha},L}(x,\gamma)+h_4\psi_{\beta,L}(x,\gamma), & (x<0),\\ \psi_{4,I}(x,\gamma), & (0<x<d_i),\\ \psi_{\overline{\alpha},R}(x,\gamma)+a_4\psi_{\alpha,R}(x,\gamma)+b_4\psi_{\overline{\beta},R}(x,\gamma), & (x>d_i),\end{cases} \tag{19}$$

where j expresses the indices L and R, and wave functions $\psi_{\alpha,j}(x,\gamma)$, $\psi_{\overline{\alpha},j}(x,\gamma)$, $\psi_{\beta,j}(x,\gamma)$, $\psi_{\overline{\beta},j}(x,\gamma)$, and $\psi_{l,I}(x,\gamma)$ are given as

$$\psi_{\alpha,j}(x,\gamma)=\begin{pmatrix} u_j\exp(i\phi_j/2) \\ v_j\exp(-i\phi_j/2)\end{pmatrix} \times\exp\left[i\left(k_F\cos\gamma+\frac{m\Omega_{j,+}}{\hbar^2k_F\cos\gamma}\right)x\right], \quad (20)$$

$$\psi_{\overline{\alpha},j}(x,\gamma)=\begin{pmatrix} v_j\exp(i\phi_j/2) \\ u_j\exp(-i\phi_j/2)\end{pmatrix} \times\exp\left[i\left(k_F\cos\gamma-\frac{m\Omega_{j,+}}{\hbar^2k_F\cos\gamma}\right)x\right], \quad (21)$$

$$\psi_{\beta,j}(x,\gamma)=\begin{pmatrix} \tilde{u}_j\exp(i\tilde{\phi}_j/2) \\ \tilde{v}_j\exp(-i\tilde{\phi}_j/2)\end{pmatrix} \times\exp\left[-i\left(k_F\cos\gamma+\frac{m\Omega_{j,-}}{\hbar^2k_F\cos\gamma}\right)x\right], \quad (22)$$

$$\psi_{\overline{\beta},j}(x,\gamma)=\begin{pmatrix} \tilde{v}_j\exp(i\tilde{\phi}_j/2) \\ \tilde{u}_j\exp(-i\tilde{\phi}_j/2)\end{pmatrix} \times\exp\left[-i\left(k_F\cos\gamma-\frac{m\Omega_{j,-}}{\hbar^2k_F\cos\gamma}\right)x\right], \quad (23)$$

and

$$\psi_{l,l}(x,\gamma)=\begin{pmatrix} c_l\exp(-\lambda x)+d_l\exp(\lambda x) \\ e_l\exp(-\lambda x)+f_l\exp(\lambda x)\end{pmatrix} \quad (l=1,\ldots,4), \quad (24)$$

with

$$u_j=\sqrt{\frac{1}{2}\left(1+\frac{\Omega_{j,+}}{E}\right)}, \quad v_j=\sqrt{\frac{1}{2}\left(1-\frac{\Omega_{j,+}}{E}\right)},$$

$$\tilde{u}_j=\sqrt{\frac{1}{2}\left(1+\frac{\Omega_{j,-}}{E}\right)}, \quad \tilde{v}_j=\sqrt{\frac{1}{2}\left(1-\frac{\Omega_{j,-}}{E}\right)}, \quad (25)$$

$$\Omega_{j,+}=\sqrt{E^2-|\Delta_j(\gamma_+)|^2}, \quad \Omega_{j,-}=\sqrt{E^2-|\Delta_j(\gamma_-)|^2},$$

$$\lambda=\sqrt{\frac{2mU_0}{\hbar^2}-k_F^2\cos^2\gamma}, \quad (26)$$

and

$$\exp(i\phi_j)=\frac{\overline{\Delta_j}(\gamma_+)}{|\Delta_j(\gamma_+)|}\exp(i\varphi_j),$$

$$\exp(i\tilde{\phi}_j)=\frac{\overline{\Delta_j}(\gamma_-)}{|\Delta_j(\gamma_-)|}\exp(i\varphi_j). \quad (27)$$

Here we have assumed the relation $U_0,\ E_{Fx}\gg|\Omega_{j,\pm}|$. The wave functions satisfy the boundary conditions

$$\mathbf{\Psi}_l(\mathbf{x})=\begin{pmatrix}\mathbf{u}_l(\mathbf{x}) \\ \mathbf{v}_l(\mathbf{x})\end{pmatrix}, \quad \mathbf{\Psi}_l(\mathbf{x})|_{x=0_-}=\mathbf{\Psi}_l(\mathbf{x})|_{x=0_+},$$

$$\left.\frac{d\mathbf{\Psi}_l(\mathbf{x})}{dx}\right|_{x=0_-}=\left.\frac{d\mathbf{\Psi}_l(\mathbf{x})}{dx}\right|_{x=0_+}, \quad (28)$$

$$\mathbf{\Psi}_l(\mathbf{x})|_{x=d_{i,-}}=\mathbf{\Psi}_l(\mathbf{x})|_{x=d_{i,+}},$$

$$\left.\frac{d\mathbf{\Psi}_l(\mathbf{x})}{dx}\right|_{x=d_{i,-}}=\left.\frac{d\mathbf{\Psi}_l(\mathbf{x})}{dx}\right|_{x=d_{i,+}}. \quad (29)$$

From the conjugate processes of the above four wave functions, we obtain another set of wave functions $\hat{\Psi}_l(\mathbf{x})$ $(l=1,\ldots,4)$ which satisfy

$$\int d\mathbf{x}_1\hat{\Psi}_l^t(\mathbf{x}_1)\check{H}(\mathbf{x}_1,\mathbf{x}_2)=E\hat{\Psi}_l^t(\mathbf{x}_2), \quad \hat{\Psi}_l(\mathbf{x}_2)=\begin{pmatrix}\hat{\mathbf{u}}(\mathbf{x}_2) \\ \hat{\mathbf{v}}(\mathbf{x}_2)\end{pmatrix}, \quad (30)$$

$$E\hat{u}(\mathbf{x}_2)=h_0\hat{u}(\mathbf{x}_2)+\int d\mathbf{x}_1\Delta^*(\mathbf{s},\mathbf{r})\hat{v}(\mathbf{x}_1),$$

$$E\hat{v}(\mathbf{x}_2)=-h_0\hat{v}(\mathbf{x}_2)+\int d\mathbf{x}_1\Delta(\mathbf{s},\mathbf{r})\hat{u}(\mathbf{x}_1). \quad (31)$$

For an energy $E>(\max[|\overline{\Delta_R}(\gamma_+)|,|\overline{\Delta_R}(\gamma_-)|,|\overline{\Delta_L}(\gamma_+)|, |\Delta_L(\gamma_-)|])$, $\hat{\Psi}_l(\mathbf{x})$ corresponds to the four elementary processes shown in Fig. 2 of Ref. 41. They also satisfy the boundary conditions given by Eqs. (28) and (29). As in the case of $\hat{\Psi}_l(\mathbf{x})$, $\hat{\Psi}_l(\mathbf{x})$ can also be written as

$$\hat{\Psi}_l(\mathbf{x})=\exp(-ik_Fy\sin\gamma)\hat{\Psi}_l(x,\gamma). \quad (32)$$

The explicit forms of these functions are not written here for brevity. Using the eight wave functions, Green's function is then expressed as

$$\mathbf{G}(x,x',k_y,E)=\begin{cases}\alpha_1\Psi_3(x,\gamma)\hat{\Psi}_1^t(x',\gamma)+\alpha_2\Psi_3(x,\gamma)\hat{\Psi}_2^t(x',\gamma)+\alpha_3\Psi_4(x,\gamma)\hat{\Psi}_1^t(x',\gamma)+\alpha_4\Psi_4(x,\gamma)\hat{\Psi}_2^t(x',\gamma), & x<x', \\ \beta_1\Psi_1(x,\gamma)\hat{\Psi}_3^t(x',\gamma)+\beta_2\Psi_2(x,\gamma)\hat{\Psi}_3^t(x',\gamma)+\beta_3\Psi_1(x,\gamma)\hat{\Psi}_4^t(x',\gamma)+\beta_4\Psi_2(x,\gamma)\hat{\Psi}_4^t(x',\gamma), & x>x',\end{cases} \quad (33)$$

$$\mathbf{G}(x,x',k_y,E)=\left(\frac{m}{i\hbar^2k_{Fx}}\right)\left\{\frac{1}{\Omega_{L,+}}\exp[ik_{L,+}(x-x')]\mathbf{A}+\frac{1}{\Omega_{L,-}}\exp[-i\tilde{k}_{L,-}(x-x')]\mathbf{B}+\frac{\tilde{a}_1}{\Omega_{L,-}}\exp[-i(\tilde{k}_{L,+}x-\tilde{k}_{L,-}x')]\mathbf{C}\right.$$
$$\left.+\frac{a_1}{\Omega_{L,+}}\exp[i(k_{L,-}x-k_{L,+}x')]\mathbf{D}\right\}, \quad x>x', \quad (34)$$

$$\mathbf{G}(x,x',k_y,E)=\left(\frac{m}{i\hbar^2 k_{Fx}}\right)\left\{\frac{1}{\Omega_{L,-}}\exp[-i\tilde{k}_{L,-}(x-x')]\tilde{\mathbf{A}}+\frac{1}{\Omega_{L,+}}\exp[ik_{L,+}(x-x')]\tilde{\mathbf{B}}+\frac{\tilde{a}_1}{\Omega_{L,-}}\exp[-i(\tilde{k}_{L,+}x-\tilde{k}_{L,-}x')]\mathbf{C}\right.$$
$$\left.+\frac{a_1}{\Omega_{L,+}}\exp[i(k_{L,-}x-k_{L,+}x')]\mathbf{D}\right\},\quad x'>x. \tag{35}$$

In the above, we have neglected the term which includes the atomic scale oscillations. The 2×2 matrices **A**, **B**, $\tilde{\mathbf{A}}$, $\tilde{\mathbf{B}}$, **C**, and **D** are given as

$$\mathbf{A}=\begin{pmatrix}u_L^2, & u_Lv_L\exp(i\phi_L)\\ u_Lv_L\exp(-i\phi_L) & v_L^2\end{pmatrix},\quad \mathbf{B}=\begin{pmatrix}\tilde{v}_L^2, & \tilde{u}_L\tilde{v}_L\exp(i\tilde{\phi}_L)\\ \tilde{u}_L\tilde{v}_L\exp(-i\tilde{\phi}_L) & \tilde{u}_L^2\end{pmatrix}, \tag{36}$$

$$\tilde{\mathbf{A}}=\begin{pmatrix}\tilde{u}_L^2, & \tilde{u}_L\tilde{v}_L\exp(i\tilde{\phi}_L)\\ \tilde{u}_L\tilde{v}_L\exp(-i\tilde{\phi}_L) & \tilde{v}_L^2\end{pmatrix},\quad \tilde{\mathbf{B}}=\begin{pmatrix}v_L^2, & u_Lv_L\exp(i\phi_L)\\ u_Lv_L\exp(-i\phi_L) & u_L^2\end{pmatrix}, \tag{37}$$

$$\mathbf{C}=\begin{pmatrix}\tilde{u}_L\tilde{v}_L & \tilde{u}_L^2\exp(i\tilde{\phi}_L)\\ \tilde{v}_L^2\exp(-i\tilde{\phi}_L) & \tilde{u}_L\tilde{v}_L\end{pmatrix},\quad \mathbf{D}=\begin{pmatrix}u_Lv_L & v_L^2\exp(i\phi_L)\\ u_L^2\exp(-i\phi_L) & u_Lv_L\end{pmatrix}, \tag{38}$$

with

$$k_L^{\pm}=\left(k_F\cos\gamma\pm\frac{m\Omega_{L,+}}{\hbar^2k_F\cos\gamma}\right),\quad \tilde{k}_L^{\pm}=\left(k_F\cos\gamma\pm\frac{m\Omega_{L,-}}{\hbar^2k_F\cos\gamma}\right). \tag{39}$$

In the above, a_1 and $\tilde{a}_1$ are expressed as

$$a_1=-\frac{\Gamma_A\Gamma_B(1-\sigma_N)+\sigma_N\Gamma_C\Gamma_D}{\Gamma_A\Gamma_E(1-\sigma_N)+\sigma_N\Gamma_C\Gamma_F},\quad \tilde{a}_1=-\frac{\tilde{\Gamma}_A\tilde{\Gamma}_B(1-\sigma_N)+\sigma_N\tilde{\Gamma}_C\tilde{\Gamma}_D}{\tilde{\Gamma}_A\tilde{\Gamma}_E(1-\sigma_N)+\sigma_N\tilde{\Gamma}_C\tilde{\Gamma}_F}, \tag{40}$$

with

$$\Gamma_A=1-\Gamma_{R,+}\Gamma_{R,-}\gamma_3\gamma_4,\quad \Gamma_B=\Gamma_{L,+}-\Gamma_{L,-}\gamma_1\gamma_2,\quad \Gamma_C=1-\Gamma_{L,-}\Gamma_{R,-}\gamma_2\gamma_4\exp(-i\varphi), \tag{41}$$

$$\Gamma_D=\Gamma_{L,+}-\Gamma_{R,+}\gamma_1\gamma_3\exp(i\varphi),\quad \Gamma_E=1-\Gamma_{L,+}\Gamma_{L,-}\gamma_1\gamma_2,\quad \Gamma_F=1-\Gamma_{L,+}\Gamma_{R,+}\gamma_1\gamma_3\exp(i\varphi), \tag{42}$$

and

$$\tilde{\Gamma}_A=\Gamma_A,\quad \tilde{\Gamma}_B=\Gamma_{L,-}-\Gamma_{L,+}\gamma_1\gamma_2,\quad \tilde{\Gamma}_C=\Gamma_F,\quad \tilde{\Gamma}_D=\Gamma_{L,-}-\Gamma_{R,-}\gamma_2\gamma_4\exp(-i\varphi), \tag{43}$$

$$\tilde{\Gamma}_E=\Gamma_E,\quad \tilde{\Gamma}_F=\Gamma_C,\quad \Gamma_{L,\pm}=\frac{|\overline{\Delta}_L(\gamma_\pm)|}{E+\Omega_{L,\pm}},\quad \Gamma_{R,\pm}=\frac{|\overline{\Delta}_R(\gamma_\pm)|}{E+\Omega_{R,\pm}}. \tag{44}$$

The quantities γ_i $(i=1,\ldots,4)$ are expressed as

$$\gamma_1=\frac{\overline{\Delta}_L(\theta_+)}{|\overline{\Delta}_L(\theta_+)|},\quad \gamma_2=\frac{|\overline{\Delta}_L(\theta_-)|}{\overline{\Delta}_L(\theta_-)},\quad \gamma_3=\frac{|\overline{\Delta}_R(\theta_+)|}{\overline{\Delta}_R(\theta_+)},\quad \gamma_4=\frac{\overline{\Delta}_R(\theta_-)}{|\overline{\Delta}_R(\theta_-)|}. \tag{45}$$

After an analytical continuation from E to $i\omega_n$, where $\omega_n=2\pi k_BT(n+1/2)$ denotes the Matsubara frequency, $\mathrm{Tr}\{\mathbf{G}(x,x',k_y,i\omega_n)\}$ is obtained. By assuming $E_{Fx}\gg|\Delta_j(\theta_\pm)|$ $(j=L,R)$, the Josephson current $I(\varphi)$ is obtained as[64]

$$R_NI(\varphi)=\frac{\pi\overline{R_N}k_BT}{e}\left\{\sum_{\omega_n}\int_{-\pi/2}^{\pi/2}\left[\frac{a_1(\theta,i\omega_n,\varphi)}{\Omega_{n,L,+}}\left|\overline{\Delta}_L(\theta_+)\right|-\frac{\tilde{a}_1(\theta,i\omega_n,\varphi)}{\Omega_{n,L,-}}\left|\overline{\Delta}_L(\theta_-)\right|\right]\cos\theta\,d\theta\right\}, \tag{46}$$

where $\Omega_{n,L,\pm}=\mathrm{sgn}(\omega_n)\sqrt{\Delta_L^2(\theta_\pm)+\omega_n^2}$. The quantity R_N denotes the normal resistance and $\overline{R_N}$ is expressed as

$$\overline{R_N}^{-1}=\int_{-\pi/2}^{\pi/2}\sigma_N\cos\theta\,d\theta,\quad \sigma_N=\frac{4Z_\theta^2}{(1-Z_\theta^2)^2\sinh^2(\lambda d_i)+4Z_\theta^2\cosh^2(\lambda d_i)}, \tag{47}$$

$$\lambda=(1-\kappa^2\cos^2\theta)^{1/2}\lambda_0,\quad Z_\theta=\frac{\kappa\cos\theta}{\sqrt{1-\kappa^2\cos^2\theta}}, \tag{48}$$

where we have introduced two parameters $\lambda_0=\sqrt{2mU_0/\hbar^2}$ and $\kappa=k_F/\lambda_0$. Here σ_N denotes the tunneling conductance for the injected quasiparticle when the junction is in the normal state. In the above, $a_1(\theta,i\omega_n,\varphi)$ and $\tilde{a}_1(\theta,i\omega_n,\varphi)$ are given as

$$a_1(\theta,i\omega_n,\varphi)=i\,\frac{\Gamma_2(\theta,i\omega_n)\Gamma_5(\theta,i\omega_n)(1-\sigma_N)+\sigma_N\Gamma_6(\theta,i\omega_n,\varphi)\Gamma_3(\theta,i\omega_n,\varphi)}{\Gamma_1(\theta,i\omega_n)\Gamma_2(\theta,i\omega_n)(1-\sigma_N)+\sigma_N\Gamma_3(\theta,i\omega_n,\varphi)\Gamma_4(\theta,i\omega_n,\varphi)}, \tag{49}$$

$$\tilde{a}_1(\theta,i\omega_n,\varphi)=i\,\frac{\Gamma_2(\theta,i\omega_n)\Gamma_7(\theta,i\omega_n)(1-\sigma_N)+\sigma_N\Gamma_8(\theta,i\omega_n,\varphi)\Gamma_4(\theta,i\omega_n,\varphi)}{\Gamma_1(\theta,i\omega_n)\Gamma_2(\theta,i\omega_n)(1-\sigma_N)+\sigma_N\Gamma_3(\theta,i\omega_n,\varphi)\Gamma_4(\theta,i\omega_n,\varphi)}, \tag{50}$$

with

$$\Gamma_1(\theta,i\omega_n)=1+\eta_{L,+}\eta_{L,-},\quad \Gamma_2(\theta,i\omega_n)=1+\eta_{R,+}\eta_{R,-},\quad \eta_{L(R),\pm}=\frac{\overline{\Delta}_{L(R)}(\theta_\pm)}{\omega_n+\Omega_{n,L(R),\pm}}, \tag{51}$$

$$\Gamma_3(\theta,i\omega_n,\varphi)=1+\eta_{L,-}\eta_{R,-}\exp(-i\varphi),\quad \Gamma_4(\theta,i\omega_n,\varphi)=1+\eta_{L,+}\eta_{R,+}\exp(i\varphi), \tag{52}$$

$$\Gamma_5(\theta,i\omega_n)=\Gamma_{n,L,+}-\Gamma_{n,L,-}\exp[i(\alpha_+-\alpha_-)],\quad \Gamma_6(\theta,i\omega_n,\varphi)=\Gamma_{n,L,+}-\Gamma_{n,R,+}\exp[i(\varphi+\alpha_+-\beta_+)], \tag{53}$$

$$\Gamma_7(\theta,i\omega_n)=\Gamma_{n,L,-}-\Gamma_{n,L,+}\exp[i(\alpha_+-\alpha_-)],\quad \Gamma_8(\theta,i\omega_n,\varphi)=\Gamma_{n,L,-}-\Gamma_{n,R,-}\exp[i(-\varphi-\alpha_-+\beta_-)], \tag{54}$$

$$\Gamma_{n,L,\pm}=\frac{\mathrm{sgn}(\omega_n)|\overline{\Delta}_L(\gamma_\pm)|}{\omega_n+\Omega_{n,L,\pm}},\quad \Gamma_{n,R,\pm}=\frac{\mathrm{sgn}(\omega_n)|\overline{\Delta}_R(\gamma_\pm)|}{\omega_n+\Omega_{n,R,\pm}},\quad \Omega_{n,R,\pm}=\mathrm{sgn}(\omega_n)\sqrt{\Delta_R^2(\theta_\pm)+\omega_n^2}, \tag{55}$$

$$\exp(i\alpha_+)=\gamma_1,\quad \exp(-i\alpha_-)=\gamma_2,\quad \exp(-i\beta_+)=\gamma_3,\quad \exp(i\beta_-)=\gamma_4. \tag{56}$$

After straightforward calculations, we finally obtain the formula for the Josephson current as

$$R_NI(\varphi)=\frac{\pi\overline{R_N}k_BT}{e}\left\{\sum_{\omega_n}\int_{-\pi/2}^{\pi/2}\overline{F}(\theta,i\omega_n,\varphi)\sigma_N\cos\theta\,d\theta\right\}, \tag{57}$$

$$\overline{F}(\theta,i\omega_n,\varphi)=4\Gamma_{n,L,+}\Gamma_{n,R,+}\times\frac{[(1-\sigma_N)|\Gamma_1(\theta,i\omega_n)\Gamma_2(\theta,i\omega_n)|\sin(\varphi+\alpha_+-\beta_+-\Psi_b)+\sigma_N|\Gamma_3(\theta,i\omega_n,\varphi)|^2\sin(\varphi+\alpha_+-\beta_+)]}{|(1-\sigma_N)\Gamma_1(\theta,i\omega_n)\Gamma_2(\theta,i\omega_n)+\sigma_N\Gamma_3(\theta,i\omega_n,\varphi)\Gamma_4(\theta,i\omega_n,\varphi)|^2}, \tag{58}$$

$$\exp(i\Psi_b)=\frac{\Gamma_1(\theta,i\omega_n)\Gamma_2(\theta,i\omega_n)}{|\Gamma_1(\theta,i\omega_n)\Gamma_2(\theta,i\omega_n)|}. \tag{59}$$

When $\sigma_N\to 0$, this formula is simplified and the resultant $R_NI(\varphi)$ becomes

$$\begin{aligned}R_NI(\varphi)&=\frac{\pi\overline{R_N}k_BT}{e}\left\{\sum_{\omega_n}\int_{-\pi/2}^{\pi/2}\frac{4\sin(\varphi+\alpha_+-\beta_+-\Psi_b)\Gamma_{n,L,+}\Gamma_{n,R,+}}{|\Gamma_1(\theta,i\omega_n)\Gamma_2(\theta,i\omega_n)|}\,\sigma_N\cos\theta\,d\theta\right\}\\&=\frac{\pi\overline{R_N}k_BT}{e}\left\{\sum_{\omega_n}\int_{-\pi/2}^{\pi/2}\mathrm{Im}\left[\frac{4\exp(i\varphi)\eta_{L,+}\eta_{R,+}}{\Gamma_1(\theta,i\omega_n)\Gamma_2(\theta,i\omega_n)}\,\sigma_N\cos\,\theta\,d\theta\right]\right\}.\end{aligned} \tag{60}$$

Also, $\mathbf{G}_{12}(0,0,k_y,i\omega_n)$ and $\mathbf{G}_{21}(d_i,d_i,k_y,i\omega_n)$ are given as

$$\mathbf{G}_{12}(0,0,k_y,i\omega_n)=-\left(\frac{m}{k_{Fx}\hbar^2}\right)\frac{2\eta_{L,+}\exp(i\varphi_L)}{1+\eta_{L,+}\eta_{L,-}}, \tag{61}$$

$$\mathbf{G}_{21}(d_i,d_i,k_y,i\omega_n)=-\left(\frac{m}{k_{Fx}\hbar^2}\right)\frac{2\eta_{R,+}\exp(-i\varphi_R)}{1+\eta_{R,+}\eta_{R,-}}. \tag{62}$$

Since the θ component of the local density of states of quasiparticles in the normal states, $\rho_N(\theta)$, is given as $\rho_N(\theta)=(m/\pi k_{Fx}\hbar^2)$, Eq. (60) can be rewritten as

$$R_NI(\varphi)=\frac{\pi\overline{R_N}k_BT}{e}\left\{\sum_{\omega_n}\int_{-\pi/2}^{\pi/2}\mathrm{Im}[\mathbf{G}_{12}(0,0,k_y,i\omega_n)\mathbf{G}_{21}(d_i,d_i,k_y,i\omega_n)]t(\theta)\cos\theta\,d\theta\right\}. \tag{63}$$

In the above, $t(\theta)$ $[t(\theta)=\sigma_N(\theta)/(\rho_N^2(\theta)\pi^2)]$ denotes the matrix element of the tunneling Hamiltonian. The quantity $\mathbf{G}_{12}(0,0,k_y,i\omega_n)$ $[\mathbf{G}_{21}(d_i,d_i,k_y,i\omega_n)]$ expresses the anomalous Green's function [conjugate of the anomalous Green's function] at the interface of the left [right] side of the superconductor and can be regarded as the ω_n and k_y component of the pair amplitude at the interface of the left [right] superconductor. The pair amplitude at the interface does not represent those of bulk superconductor in general.

When the time-reversal symmetry is not broken, $\overline{\Delta}_{L(R)}(\theta_\pm)$ is chosen as real quantities. Consequently, Eq. (57) can be simplified as[64]

$$R_N I(\varphi)=\frac{\pi \overline{R_N} k_B T}{e}\left\{\sum_{\omega_n}\int_{-\pi/2}^{\pi/2} F(\theta,i\omega_n,\varphi)\sin\varphi\,\sigma_N\cos\theta\,d\theta\right\}, \tag{64}$$

$$F(\theta,i\omega_n,\varphi)=\frac{4\eta_{L,+}\eta_{R,+}[(1-\sigma_N)\Gamma_1(\theta,i\omega_n)\Gamma_2(\theta,i\omega_n)+\sigma_N|\Gamma_3(\theta,i\omega_n,\varphi)|^2]}{|(1-\sigma_N)\Gamma_1(\theta,i\omega_n)\Gamma_2(\theta,i\omega_n)+\sigma_N\Gamma_3(\theta,i\omega_n,\varphi)\Gamma_4(\theta,i\omega_n,\varphi)|^2}. \tag{65}$$

In the following, we will survey the intrinsic properties of the formulation [Eqs. (57) and (64)]. First, Eq. (57) can be applied to Josephson junctions whose electrodes have pairing symmetries which break time-reversal symmetry: i.e., $\overline{\Delta}_{L(R)}(\theta_\pm)$ becomes complex. In general, $I(\varphi)$ can be decomposed into the series of $\sin(n\varphi)$ and $\cos(n\varphi)$,

$$I(\varphi)=\sum_{n\geqslant 1}[I_n\sin(n\varphi)+J_n\cos(n\varphi)]. \tag{66}$$

When the time-reversal symmetry is not broken, J_n $(n\geqslant 1)$ vanishes. Second, the formula includes the Josephson current component carried by the multiple reflection process at the interface. In the above equation, the current components with index n correspond to the amplitudes of the nth reflection processes of quasiparticles. Third, the formula naturally includes the bound-state condition in the denominator of $F(\theta,i\omega_n,\varphi)$ or $F(\theta,i\omega_n,\varphi)$, which we will refer to as $F_d(\theta,i\omega_n,\varphi)$. If we replace $i\omega_n$ with E, the condition $F_d(\theta,E,\varphi)=0$ can be regarded as a linear combination of two types of bound-state conditions. For a high-conductance junction $(\sigma_N\rightarrow 1)$, the condition $F_d(\theta,E,\varphi)\approx\Gamma_3(\theta,E,\varphi)\Gamma_4(\theta,E,\varphi)=0$ gives the energy levels of bound states formed between the diagonal pair potentials due to the Andreev-reflection process. For a low-conductance junction $(\sigma_N\rightarrow 0)$, the condition $F_d(\theta,E,\varphi)\approx\Gamma_1(\theta,E)\Gamma_2(\theta,E)=0$ gives the energy levels of bound states formed around the surfaces of isolated semi-infinite superconductors. Fourth, in Eq. (64), for a fixed φ, the direction of the current becomes either positive or negative depending on the angle. The sign of $F(\theta,i\omega_n,\varphi)$ is determined by the sign of the numerator, i.e., the sign of $\Delta_R(\theta_+)\Delta_L(\theta_+)$. The total Josephson current is regarded as the integration of all θ components. This is one of the important properties of the Josephson junction in anisotropic superconductors: the sign change of the pair potential on the Fermi surface.

Finally, Eqs. (57) and (64) are consistent with the previous formulas for the Josephson current as limiting cases. When the left and the right superconductors are s-wave superconductors with the same magnitude of the pair potential, we can choose $\overline{\Delta}_L(\theta_\pm)=\overline{\Delta}_R(\theta_\pm)=\Delta_0(T)$ and $\Omega_{n,L,\pm}=\Omega_{n,R,\pm}=\Omega_0=\sqrt{\Delta_0^2(T)+\omega_n^2}$. The resulting $F(\theta,i\omega_n,\varphi)$ is expressed as

$$F(\theta,i\omega_n,\varphi)=\frac{4\Delta_0^2(T)}{4(1-\sigma_N)\Omega_0^2+\sigma_N|(\omega_n+\Omega_0)+(\Omega_0-\omega_n)\exp(-i\varphi)|^2}. \tag{67}$$

Performing the summation of the Matsubara frequency analytically, $R_N I(\varphi)$ is expressed as[78,79]

$$R_N I(\varphi)=\frac{\pi\overline{R_N}}{e}\int_{-\pi/2}^{\pi/2}\frac{\Delta_0(T)}{2\sqrt{1-\sigma_N\sin^2(\varphi/2)}}\tanh\left(\frac{\Delta_0(T)\sqrt{1-\sigma_N\sin^2(\varphi/2)}}{2k_BT}\right)\sigma_N\cos\theta\,\sin\varphi\,d\theta. \tag{68}$$

For $\sigma_N\sim 0$, $I(\varphi)$ is proportional to $\sin(\varphi)$ and the results of Ambegaokar-Baratoff (AB) theory[82] is reproduced, while, for $\sigma_N=1$, Eq. (68) reproduces the previous results by Kulik and Ome'lyanchuk.[66] When the left and right superconductors are d-wave superconductors, four pair potentials are chosen as $\overline{\Delta}_L(\theta_\pm)=\Delta_d(T)\cos[2(\theta\mp\alpha)]$ and $\overline{\Delta}_R(\theta_\pm)=\Delta_d(T)\cos[2(\theta\mp\beta)]$. If we only take into account the $\theta=0$ component of $F(\theta,i\omega_n,\varphi)$ in the θ integral of Eq. (64), we reproduce the Sigrist-Rice results[11] where $R_N I(\varphi)$ is proportional to $\cos(2\alpha)\cos(2\beta)$. When σ_N is set equal to unity, we can obtain the previous results by Yip[26] in pin-hole geometry. In the following sections, the Josephson junction in the various cases will be investigated in detail.

III. JOSEPHSON EFFECT IN $s/I/d$ JUNCTIONS

In this section, the properties of the Josephson effect between s-wave superconductor and d-wave superconductor junctions are discussed. Since the symmetry of the pair potential in the left and right superconductors is different, it is not evident whether the amplitude of the Josephson current is nonzero or not. To reveal it, we have developed a microscopic theory of the Josephson effect in an s-wave superconductor/insulator/$d_{x^2-y^2}$-wave superconductor junction.[22] However, the previous theory is applicable only when the interface is parallel to the crystal axes. In the following, more general cases are discussed using the formula presented in the previous section.

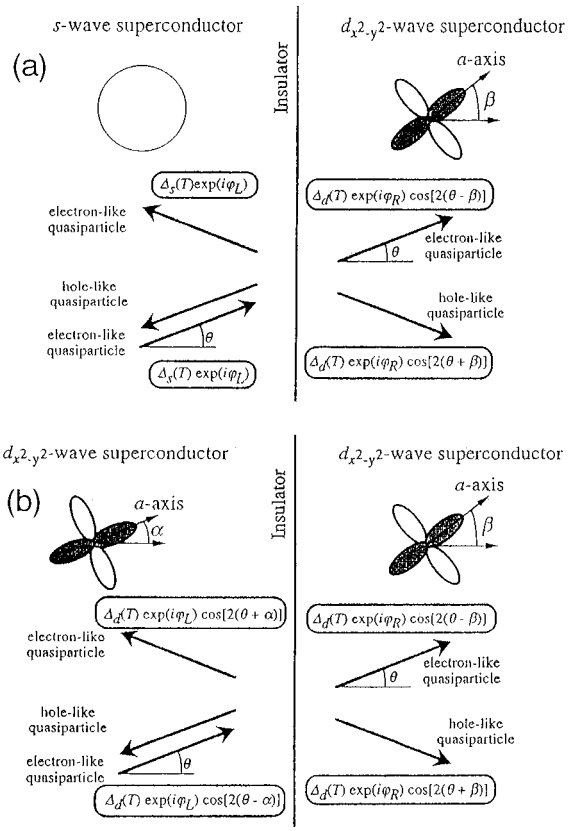

FIG. 1. Schematic illustration of reflection and transmission of quasiparticles at the interface: (a) s-wave superconductor/insulator/$d_{x^2-y^2}$-wave superconductor ($s/I/d$) junction. (b) $d_{x^2-y^2}$-wave superconductor/insulator/$d_{x^2-y^2}$-wave superconductor ($d/I/d$) junction.

We consider the case when the ab plane of the $d_{x^2-y^2}$-wave superconductor is in the plane as shown in Fig. 1(a). The quantity β expresses the angle between the normal to the interface and the crystal axis (a axis) of the $d_{x^2-y^2}$-wave superconductor. For a quasiparticle injection with angle θ to the interface normal, the three effective pair potentials participate in this process. The most essential point is that the transmitted electronlike quasiparticle and holelike quasiparticle do not always ''feel'' the same pair potentials. In such a situation, $\Delta_L(\theta_\pm)$ and $\Delta_R(\theta_\pm)$ are given as $\Delta_s(T)$ and $\Delta_d(T)\cos[2(\theta\mp\beta)]$, respectively. The quantities $\eta_{L,+}$ and $\eta_{L,-}$ in Eq. (51) are substituted by

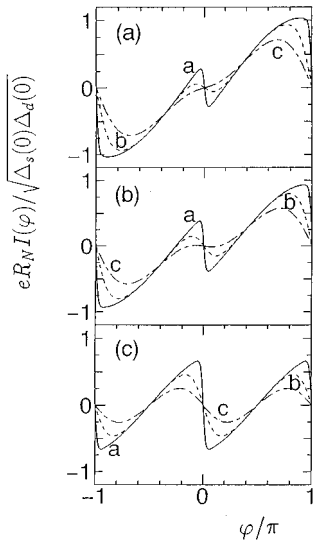

FIG. 2. Josephson current $I(\varphi)$ plotted as a function of φ for $\lambda_0 d_i=0$ and $\kappa=0.5$ with (a) $\beta=0$, (b) $\beta=\pi/8$, and (c) $\beta=\pi/4$. Curve a, $T/T_s=0.05$; b, $T/T_s=0.3$; and c, $T/T_s=0.6$.

$$\eta_{L,+}=\eta_{L,-}=\frac{\Delta_s(T)}{\omega_n+\Omega_{n,s}},$$

$$\Omega_{n,s}=\mathrm{sgn}(\omega_n)\sqrt{\omega_n^2+\Delta_s^2(T)}. \tag{69}$$

To understand the current-phase relation $I(\varphi)$ clearly, the condition for the formation of ZES's for $\sigma_N\to 0$ and the signs of $F(\theta,i\omega_n,\varphi)$ are summarized in Table I for $0\leqslant\beta\leqslant\pi/4$. Although the particular choice of T_s and T_d is not essential, we select the critical temperatures of the s-wave superconductor and d-wave superconductor as $T_s=8.8$ K ~ 0.7 meV/k_B and $T_d=90$ K~ 7.8 meV/k_B, respectively. The corresponding $\Delta_s(0)$ and $\Delta_d(0)$ are 1.2 and 18 meV. Both $\Delta_s(T)$ and $\Delta_d(T)$ are assumed to obey the BCS relation. In Figs. 2 and 3, $I(\varphi)$ is plotted for various β. Since the time-reversal symmetry holds, $J_n=0$ for ($n\geqslant 1$) and $I(\varphi)=-I(-\varphi)$ are satisfied. In the case of $\lambda_0 d_i=0$, i.e., $\sigma_N=1$ (Fig. 2) the bound states are formed between the diagonal potentials due to the multiple Andreev reflection. Since the magnitudes of I_n ($n>1$) in Eq. (66) are not negligible, $I(\varphi)$ deviates from the ordinary sinusoidal dependences. The condition for the formation of ZES's is expressed as the vanishment of $F_d(\theta,i\omega_n=0,\varphi)=0$. Since $\eta_{L,\pm}=1$, $\eta_{R,+}=\pm 1$, and $\eta_{R,-}=\pm 1$ are satisfied, $F_d(\theta,0,\varphi)$ vanishes for $\varphi=0$ and $\varphi=\pm\pi$. The existence of ZES's induces the enhancement of the Josephson current at low temperatures as

TABLE I. $0\leqslant\beta\leqslant\pi/4$. Condition for the formation of the bound states and the sign of $F(\theta,i\omega_n,\varphi)$ in the $s/I/d$ junction.

	Zero-energy states ($\sigma_N\to 0$) left side	Zero-energy states ($\sigma_N\to 0$) right side	Sign of $F(\theta,i\omega_n,\varphi)$ ($0<\varphi<\pi$)	Sign of $F(\theta,i\omega_n,\varphi)$ ($-\pi<\varphi<0$)
$\pi/4+\beta<\theta<\pi/2$	No	No	−	+
$\pi/4-\beta<\theta<\pi/4+\beta$	No	Yes	+	−
$-\pi/4+\beta<\theta<\pi/4-\beta$	No	No	+	−
$-\pi/4-\beta<\theta<-\pi/4+\beta$	No	Yes	−	+
$-\pi/2<\theta<-\pi/4-\beta$	No	No	−	+

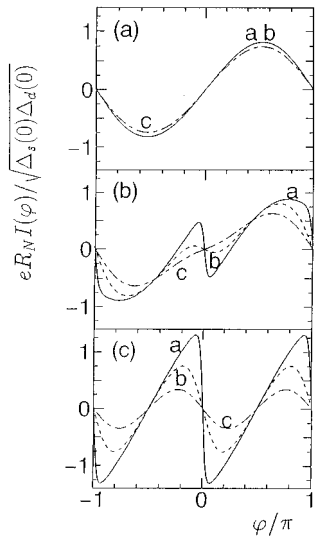

FIG. 3. Josephson current $I(\varphi)$ plotted as a function of φ for $\lambda_0 d_i=1$ and $\kappa=0.5$ with (a) $\beta=0$, (b) $\beta=\pi/8$, and (c) $\beta=\pi/4$. Curve a, $T/T_s=0.05$; b, $T/T_s=0.3$; and c, $T/T_s=0.6$.

seen in curves a in Fig. 2. Even when σ_n deviates from 1, i.e., $\lambda_0 d_i$ becomes nonzero, $F_d(\theta,0,\varphi)$ vanishes for $\varphi=0$, $\pm\pi$ for $\pm\pi/4-\beta<\theta<\pm\pi/4+\beta$. For nonzero β, ZES's are formed at the interface and the resulting $I(\varphi)$ is also enhanced around $\varphi=0$ and $\varphi=\pm\pi$ [curve a in Figs. 3(b) and 3(c)]. When β is $\pi/4$ [Figs. 2(c) and 3(c)], I_1 vanishes and the contribution of I_2 becomes dominant. This is the reason for the period of oscillation of curves in Figs. 2(c) and 3(c) not being 2π but π.

Figure 4 shows the temperature dependence of the maximum Josephson current $R_N I_C(T)$ for several cases. Without the barrier potential ($\sigma_N=1$), the magnitude of $I_C(T)$ for $\beta=0$ (curve a) is larger than the other cases, independent of temperature [Fig. 4(a)]. However, as σ_N decreases from 1, i.e., as $\lambda_0 d_i$ increases, the magnitude of $I_C(T)$ for $\beta=\pi/4$

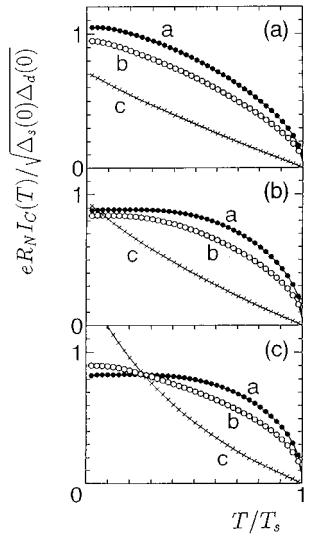

FIG. 4. Maximum Josephson current $I_C(T)$ plotted as a function of temperature for $\kappa=0.5$: (a) $\lambda_0 d_i=0$, (b) $\lambda_0 d_i=0.5$, and (c) $\lambda_0 d_i=1$. Curve a, $\beta=0$; b, $\beta=\pi/8$; and c, $\beta=\pi/4$.

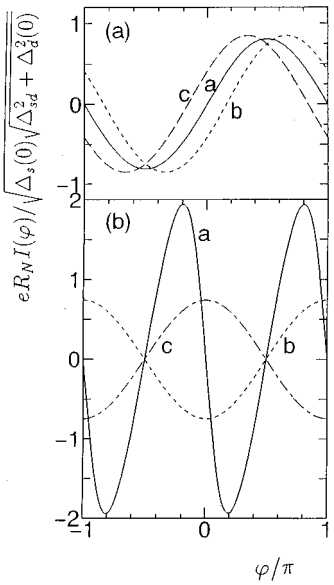

FIG. 5. Josephson current $I(\varphi)$ plotted as a function of φ for $\lambda_0 d_i=3$ and $\kappa=0.5$ with (a) $\beta=0$ and (b) $\beta=\pi/4$ at $T/T_s=0.05$. Curve a, $\Delta_{sd}=0$; b, $\Delta_{sd}=0.3\Delta_d(0)$; and c, $\Delta_{sd}=-0.3\Delta_d(0)$.

(curve c) is enhanced at low temperatures. For a low-conductance junction ($\sigma_N\to 0$), if β deviates from zero, $\overline{\Delta_R(\theta_+)}\overline{\Delta_R(\theta_-)}$ becomes negative for $\pm\pi/4-\beta<\theta<\pm\pi/4+\beta$, and $F_d(\theta,i\omega_n,\varphi)$ is reduced at low temperatures. The extreme case is when $\beta=\pi/4$, where $\overline{\Delta_R(\theta_+)}\overline{\Delta_R(\theta_-)}<0$ is satisfied for any θ. This is due to the formation of ZES's at the interface. The reduction of $F_d(\theta,i\omega_n,\varphi)$ at low temperatures is much more drastic with the decrease of σ_N, i.e., with the increase of $\lambda_0 d_i$. The resulting $I_C(T)$ is enhanced at low temperatures. Consequently, curves c in Figs. 4(b) and 4(c) have upper curvatures and are crucially different from those of the AB theory.[82] On the other hand, for $\beta=0$ and $\sigma_N\to 0$, the temperature dependence of $I_C(T)$ is similar to those obtained by AB theory.[82]

The effect of time-reversal symmetry breaking on $I(\varphi)$ is now discussed. In this case, the effective pair potentials for quasiparticles $\overline{\Delta_R(\theta_\pm)}$ are given as

$$\overline{\Delta_R(\theta_+)}=\Delta_d(T)\cos[2(\theta-\beta)]+i\Delta_{sd},$$
$$\overline{\Delta_R(\theta_-)}=\Delta_d(T)\cos[2(\theta+\beta)]+i\Delta_{sd}. \tag{70}$$

The most serious effect is that $I(\varphi)$ can no longer be expressed as a series of $\sin(n\varphi)$ any more and J_n in Eq. (66) becomes nonzero. Figure 5 shows the calculated results of $I(\varphi)$ for an s-wave superconductor/insulator/$(d_{x^2-y^2}+is)$-wave superconductor [$s/I/(d+is)$] junction when $\lambda_0 d_i=3$ and $\kappa=0.5$. For $\beta=0$, $I(\varphi)$ is expressed as a sinusoidal curve. However, $I(\varphi)=-I(-\varphi)$ is no longer satisfied due to the mixing of the s-wave component. For $\beta=\pi/4$, $I(\varphi)$ is enhanced due to the formation of ZES's as discussed above [see curve a in Fig. 5(b)]. In this case, the most dominant component in the current is I_2. By the mixing of s-wave components (curves b and c), the sign change of the pair potential felt by quasiparticles does not occur any more in the reflection process at the interface. Consequently, ZES's

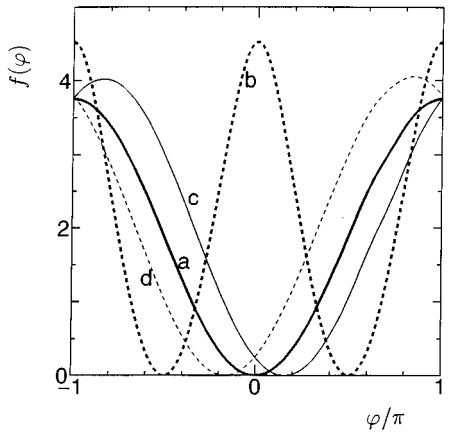

FIG. 6. Normalized free energy of the junction $f(\varphi)$ plotted as a function of φ for $\lambda_0 d_i=3$ and $\kappa=0.5$ at $T/T_s=0.05$. Curve a, $\beta=0$; $\Delta_{sd}=0$; b, $\beta=\pi/4$, $\Delta_{sd}=0$; c, $\beta=0$, $\Delta_{sd}=0.3\Delta_d(0)$; and d, $\beta=0$, $\Delta_{sd}=-0.3\Delta_d(0)$.

disappear and I_2 is drastically reduced. On the other hand, due to the existence of the s-wave component, J_1 contributes most dominantly to $I(\varphi)$ [see curves b and c in Fig. 5(b)].

We now consider the phase difference φ_0 which gives the free energy minimum. The free energy of the junction $F(\varphi)$ satisfies the relation

$$I(\varphi)=\frac{2e}{\hbar}\frac{\partial}{\partial\varphi}F(\varphi). \tag{71}$$

The dimensionless free energy $f(\varphi)$ is defined as

$$f(\varphi)=\frac{2e^2R_N}{\hbar\sqrt{\Delta_s(0)}\sqrt{\Delta_d^2(0)+\Delta_{sd}^2}}[F(\varphi)-F(\varphi_0)]. \tag{72}$$

In Fig. 6, typical line shapes of $f(\varphi)$ are plotted. When $\beta=0$, φ_0 is located at zero (curve a). This junction is a typical example of the so-called 0 junction. As the contribution of I_m $(m>1)$ to $I(\varphi)$ becomes dominant, $f(\varphi)$ has a double minimum like curve b. When $\beta=\pi/4$, the contribution of the I_1 component vanishes and φ_0 is located at $\varphi_0=\pm\pi/2$. When the s-wave component mixes, $f(\varphi)$ is not a symmetric function around the origin (see curves c and d).

Finally, we comment on the magnetic field dependence of the corner SQUID. In the corner SQUID configuration, which consists of x-axis and y-axis junctions with the same ratio, the Josephson current without magnetic field can be expressed as

$$I(\varphi)=I^{(x)}(\varphi)+I^{(y)}(\varphi), \tag{73}$$

where $I^{(x)}(\varphi)$ $[I^{(y)}(\varphi)]$ denotes the Josephson current from the x-axis [y-axis] junction. According to Eq. (66), $I^{(x)}(\varphi)$ and $I^{(y)}(\varphi)$ can be decomposed into

$$I^{(x)}(\varphi)=\sum_{n\geqslant 1}[I_n^{(x)}\sin(n\varphi)+J_n^{(x)}(n\varphi)],$$

$$I^{(y)}(\varphi)=\sum_{n\geqslant 1}[I_n^{(y)}\sin(n\varphi)+J_n^{(y)}\cos(n\varphi)]. \tag{74}$$

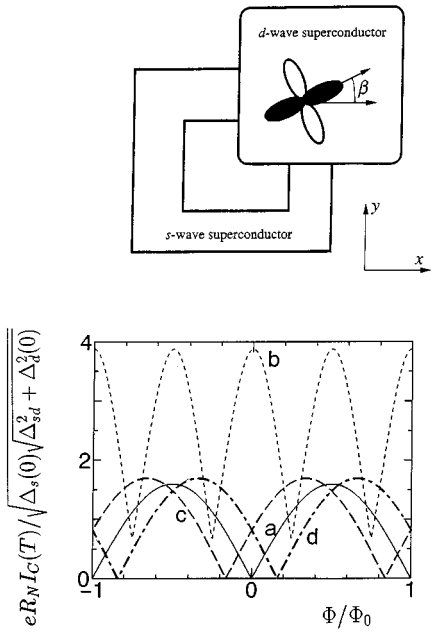

FIG. 7. Maximum Josephson current $I_C(T)$ in the corner SQUID plotted as a function of the magnetic field for $\lambda_0 d_i=3$, $\kappa=0.5$ at $T/T_s=0.05$. Curve a, $\Delta_{sd}=0$, $\beta=0$; b, $\Delta_{sd}=0$, $\beta=\pi/4$; c, $\Delta_{sd}=0.3\Delta_d(0)$, $\beta=0$; and d, $\Delta_{sd}=-0.3\Delta_d(0)$, $\beta=0$.

Following the ordinary textbook,[83] the magnetic field dependence of $I(\varphi)$ is given as

$$I(\varphi)=\sum_{n\geqslant 1}\left\{I_n^{(x)}\sin(n\varphi)+J_n^{(x)}\cos(n\varphi)\right.$$
$$\left.+I_n^{(y)}\sin\left[n\left(\varphi-\frac{2\pi\Phi}{\Phi_0}\right)\right]+J_n^{(y)}\cos\left[n\left(\varphi-\frac{2\pi\Phi}{\Phi_0}\right)\right]\right\}, \tag{75}$$

where Φ and Φ_0 denote the flux which penetrates into the SQUID and the half-unit magnetic flux quanta, respectively. In Fig. 7, the maximum total Josephson current $I_C(T)$ is plotted as a function of Φ. When β is zero, $I_C(T)$ becomes minimum at $\Phi=n\Phi_0$, where n is an integer (see curve a in Fig. 7). This anomalous magnetic field dependence is consistent with that predicted using a phenomenological theory[11] and was actually observed in experiments.[12,13] When β is $\pi/4$, the period of the oscillation becomes $0.5\Phi_0$. In this geometry, $I_C(T)$ is strongly enhanced at low temperatures due to the formation of ZES's. The experimental observation of this behavior is strongly expected to confirm our results. In the case when the s-wave component mixes, $I_C(T)$ is no longer a symmetric function of the magnetic field around the origin.

IV. JOSEPHSON EFFECT IN A $d/I/d$ JUNCTION

This section presents the properties of a d-wave superconductor/insulator/d-wave superconductor ($d/I/d$) Josephson junction. In the $d/I/d$ junction, for a quasiparticle injection from the left superconductor at an angle θ to the interface normal, four different effective pair potentials participate [Fig. 1(b)]. The four effective pair potentials are

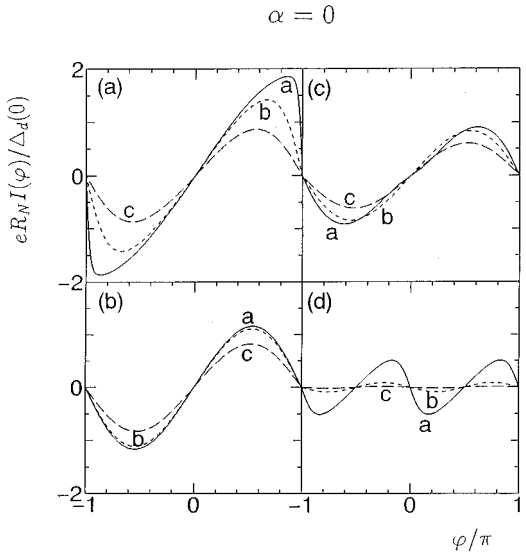

FIG. 8. Josephson current $I(\varphi)$ in a $d/I/d$ junction plotted as a function of φ for $\kappa=0.5$ and $\alpha=0$: (a) $\beta=0$, $\lambda_0 d_i=0$, (b) $\beta=0$, $\lambda_0 d_i=1$, (c) $\beta=\pi/8$, $\lambda_0 d_i=1$, and (d) $\beta=\pi/4$, $\lambda_0 d_i=1$. Curve a, $T/T_d=0.05$; b, $T/T_d=0.3$; and c, $T/T_d=0.6$.

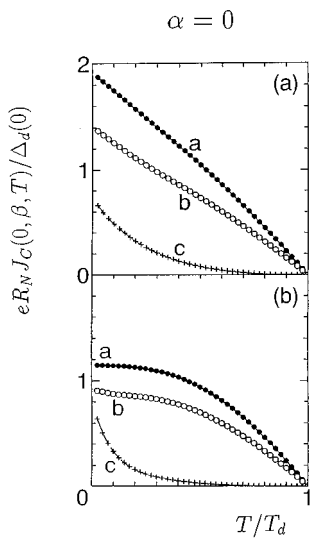

FIG. 9. Maximum Josephson current $J_C(\alpha,\beta,T)$ in a $d/I/d$ junction is plotted as a function of temperature for $\kappa=0.5$ and $\alpha=0$: (a) $\lambda_0 d_i=0$ and (b) $\lambda_0 d_i=1$. Curve a, $\beta=0$; b, $\beta=\pi/8$; and c, $\beta=\pi/4$.

$\overline{\Delta_L}(\theta_\pm)=\Delta_d(T)\cos[2(\theta\mp\alpha)]$ and $\overline{\Delta_R}(\theta_\pm)=\Delta_d(T)\cos[2(\theta\mp\beta)]$. The condition for the formation of the ZES's for $\sigma_N\to 0$ and the sign of $F(\theta,i\omega_n,\varphi)$ for various cases are shown in Tables II–IV. The Josephson current is calculated by substituting the effective pair potentials to Eq. (51). Recently, Sigrist and Rice presented a phenomenological theory (referred to as SR theory) of $I_C(T)$ in the grain boundary junctions. It predicts that the maximum Josephson current is proportional to $|\cos(2\alpha)\cos(2\beta)|$. To clarify the validity of SR theory, we define $J_C(\alpha,\beta,T)\equiv I_C(T)$ and introduce a function $B(\alpha,\beta,T)$ as

$$B(\alpha,\beta,T)=J_C(\alpha,\beta,T)/J_C(0,0,T). \tag{76}$$

In SR theory, $B(\alpha,\beta,T)$ is $|\cos(2\alpha)\cos(2\beta)|$ for every temperature. We now discuss the properties of the $d/I/d$ junction and examine the validity of AB and SR theories for three types of geometry.

First, we assume that one of the crystal axes is parallel to the interface ($\alpha=0$). Figure 8(a) shows $I(\varphi)$ of a $d/I/d$ junction with $\beta=0$ without the barrier potential ($\lambda_0 d_i=0$). In this case, I_n ($n>1$) in Eq. (66) is not negligible; that is, the contribution from the higher-order tunneling process to $I(\varphi)$ is significant. The resulting curves of $I(\varphi)$ deviate from sinusoidal shapes especially at low temperatures. With the increase of $\lambda_0 d_i$, the higher-order processes are suppressed and $I(\varphi)$ approaches the usual sinusoidal shape [Fig. 8(b)]. In the two cases corresponding to Figs. 8(a) and 8(b), $F(\theta,i\omega_n,\varphi)$, with $0<\varphi<\pi$ ($-\pi<\varphi<0$), is positive (negative), independent of θ. However, as β deviates from zero [Figs. 8(c) and 8(d)], $F(\theta,i\omega_n,\varphi)$, with $0<\varphi<\pi$ ($-\pi<\varphi<0$), becomes negative (positive) for the quasiparticle injection of θ with $\pi/4<\theta<\pi/4+\beta$ or $-\pi/4<\theta<-\pi/4+\beta$. Extreme behavior is expected when $\beta=\pi/4$, where I_1 (the lowest-order term) vanishes due to the θ integral and $I(\varphi)$ has a form close to $\sin(2\varphi)$. The temperature dependences of the maximum Josephson current $J_C(0,\beta,T)$ corresponding to the cases shown in Fig. 8 are plotted in Fig. 9. When $\beta=0$ with $\lambda_0 d_i=0$ (curve a in Fig. 9), an almost linear temperature dependence is obtained. In this case, we can perform the summation of ω_n analytically. For $\alpha=\beta=0$, where $\overline{\Delta_{L(R)}}(\theta_\pm)=\overline{\Delta_d}(T,\theta)=\Delta_d(T)\cos(2\theta)$ is satisfied, the resulting $R_N I(\varphi)$ becomes

$$R_N I(\varphi)=\frac{\pi\overline{R_N}}{e}\int_{-\pi/2}^{\pi/2}\frac{\overline{\Delta_d}(T,\theta)\sigma_N\cos\theta\,\sin\varphi}{2\sqrt{1-\sigma_N\sin^2(\varphi/2)}}\times\tanh\left[\frac{\overline{\Delta_d}(T,\theta)\sqrt{1-\sigma_N\sin^2(\varphi/2)}}{2k_BT}\right]d\theta. \tag{77}$$

For $\sigma_N\ll 1$, $R_N J_C(0,0,T)$ is expressed as

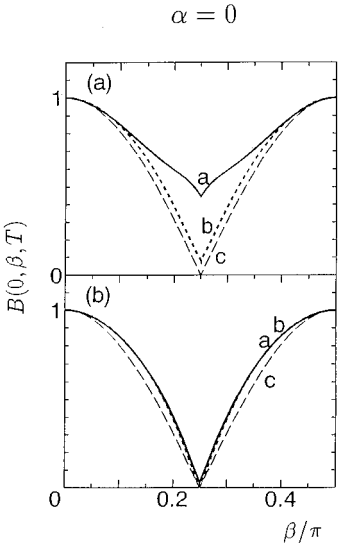

FIG. 10. $B(0,\beta,T)$ plotted as a function of β for (a) $\lambda_0 d_i=1$ and (b) $\lambda_0 d_i=3$ with $\kappa=0.5$. Curve a, $T/T_d=0.05$; b, $T/T_d=0.3$; and c, Sigrist and Rice's result (SR theory).

TABLE II. $0 \leqslant \beta \leqslant \pi/4$. Condition for the formation of the bound states and the sign of $F(\theta, i\omega_n, \varphi)$ with $\alpha = 0$ in the $d/I/d$ junction.

	Zero-energy states ($\sigma_N \to 0$) left side	Zero-energy states ($\sigma_N \to 0$) right side	Sign of $F(\theta, i\omega_n, \varphi)$ $(0 < \varphi < \pi)$	Sign of $F(\theta, i\omega_n, \varphi)$ $(-\pi < \varphi < 0)$
$\pi/4+\beta < \theta < \pi/2$	No	No	+	−
$\pi/4 < \theta < \pi/4+\beta$	No	Yes	−	+
$\pi/4-\beta < \theta < \pi/4$	No	Yes	+	−
$-\pi/4+\beta < \theta < \pi/4-\beta$	No	No	+	−
$-\pi/4 < \theta < -\pi/4+\beta$	No	Yes	−	+
$-\pi/4-\beta < \theta < -\pi/4$	No	Yes	+	−
$-\pi/2 < \theta < -\pi/4-\beta$	No	No	+	−

$$R_N J_C(0,0,T) \sim \frac{\pi \overline{R_N}}{e} \int_{-\pi/2}^{\pi/2} \frac{\overline{\Delta_d}(T,\theta)\sigma_N \cos\theta}{2} \times \tanh\left(\frac{\overline{\Delta_d}(T,\theta)}{2k_B T}\right) d\theta. \tag{78}$$

The temperature dependence of $J_C(0,0,T)$ is similar to the results of AB theory.[82] Actually, as $\lambda_0 d_i$ increases, $J_C(0,0,T)$ approaches to that of AB theory [curve a in Fig. 9(b)]. When β is nonzero, the absolute value of $J_C(0,\beta,T)$ is reduced due to the coexistence of the positive and negative values of $F(\theta, i\omega_n, \varphi)$ as a function of θ (curves b and c in Fig. 9). Anomalous behavior is noted when $\beta = \pi/4$ where $J_C(0,\beta,T)$ is rapidly enhanced due to the formation of ZES's at low temperatures (curve c in Fig. 9). In Fig. 10, $B(0,\beta,T)$ is plotted for various temperatures. Following SR theory, $B(0,\beta,T) = |\cos(2\beta)|$ is satisfied, independent of temperatures. Curve c expresses the magnitude of $|\cos(2\beta)|$ as a reference. The deviation of the magnitude of $B(0,\beta,T)$ from that of curve c is prominent around $\beta = \pi/4$ at low temperatures [curves a and b in Fig. 10(a)]. With the increase of $\lambda_0 d_i$, the deviation is drastically reduced (curves a and b). Although the effect of the formation of ZES's is completely neglected in SR theory, $B(0,\beta,T)$ is expressed by this theory fairly well for large $\lambda_0 d_i$, i.e., for small σ_N. To discuss the role of ZES's, we will define $I_z(\varphi)$, which denotes the Josephson current originating from the region C where ZES's are formed for small σ_N. The quantity $I_z(\varphi)$ is given as

$$R_N I_z(\varphi) = \frac{\pi \overline{R_N}}{e} k_B T \sum_{\omega_n} H(i\omega_n)\sin(\varphi),$$

$$H(i\omega_n) = \int_C F(\theta, i\omega_n, \varphi)\sigma_N \cos\theta \, d\theta. \tag{79}$$

As seen from Table II, the region C becomes $-\pi/4-\beta < \theta < -\pi/4+\beta$ and $\pi/4-\beta < \theta < \pi/4+\beta$. For small σ_N, $H(i\omega_n)$ becomes

$$H(i\omega_n) = \int_{\pi/4-\beta}^{\pi/4+\beta} \sigma_N \cos\theta \frac{4\eta_{L,+}(\eta_{R,+}+\eta_{R,-})}{(1+\eta_{L,+}^2)(1+\eta_{R,+}\eta_{R,-})} d\theta. \tag{80}$$

In the above, we have applied the fact that ZES's are not formed at the interface of the left superconductor since $\overline{\Delta_L}(\theta_+) = \overline{\Delta_L}(\theta_-)$ is satisfied. At low temperatures, $H(i\omega_n)$ is given as

$$H(i\omega_n) = -4 \int_{\pi/4-\beta}^{\pi/4+\beta} \frac{\cos(2\theta)}{|\cos(2\theta)|} \cos\theta \sigma_N d\theta, \tag{81}$$

and no singular behavior with respect to ω_n is expected. Consequently, the role of ZES's is not so significant.

Second, we assume the antisymmetric geometry ($\alpha = \beta$). The sign of $F(\theta, i\omega_n, \varphi)$ and the condition of the formation of ZES's for $\sigma_N \to 0$ corresponding to this geometry is shown in Table III. When σ_N is set equal to unity, i.e., $\lambda_0 d_i = 0$, the summation of the Matsubara frequency can be calculated analytically. The resulting $R_N I(\varphi)$ is expressed as

$$R_N I(\varphi) = \frac{2\pi \overline{R_N}}{e} \int_{-\pi/2}^{\pi/2} \Delta_d(0)\cos[2(\theta-\alpha)]\sin\left(\frac{\varphi}{2}\right) \times \tanh\left\{\frac{\Delta_d(0)\cos[2(\theta-\alpha)]\cos(\varphi/2)}{2k_B T}\right\} \cos\theta \, d\theta. \tag{82}$$

When $T \ll |\Delta_d(0)|$ is satisfied, the θ integration also can be performed analytically. $R_N J_C(\alpha, \alpha, T)$ becomes

TABLE III. $0 \leqslant \alpha \leqslant \pi/4$. Condition for the formation of the bound states and the sign of $F(\theta, i\omega_n, \varphi)$ with $\alpha = \beta$ in the $d/I/d$ junction.

	Zero-energy states ($\sigma_N \to 0$) left side	Zero-energy states ($\sigma_N \to 0$) right side	Sign of $F(\theta, i\omega_n, \varphi)$ $(0 < \varphi < \pi)$	Sign of $F(\theta, i\omega_n, \varphi)$ $(-\pi < \varphi < 0)$
$\pi/4+\alpha < \theta < \pi/2$	No	No	+	−
$\pi/4-\alpha < \theta < \pi/4+\alpha$	Yes	Yes	+	−
$-\pi/4+\alpha < \theta < \pi/4-\alpha$	No	No	+	−
$-\pi/4-\alpha < \theta < -\pi/4+\alpha$	Yes	Yes	+	−
$-\pi/2 < \theta < -\pi/4-\alpha$	No	No	+	−

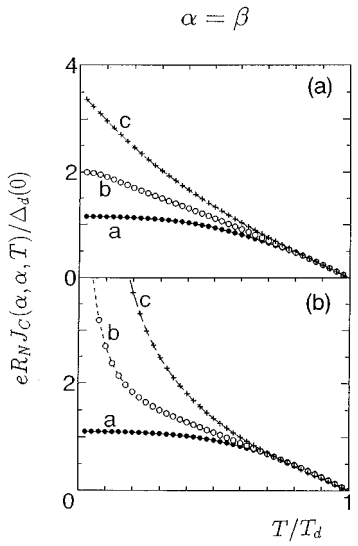

FIG. 11. Maximum Josephson current $J_C(\alpha,\beta,T)$ with $\alpha=\beta$ plotted as a function of temperature for $\kappa=0.5$: (a) $\lambda_0 d_i=1$ and (b) $\lambda_0 d_i=3$. Curve a, $\alpha=0$; b, $\alpha=\pi/8$; and c, $\alpha=\pi/4$.

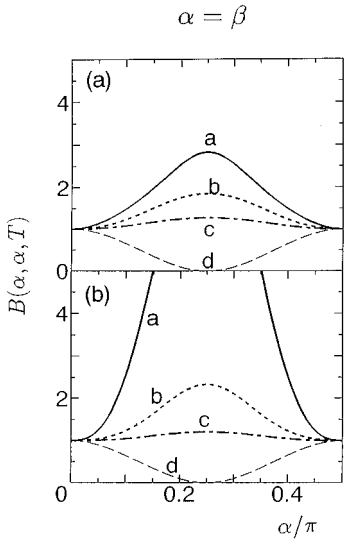

FIG. 12. $B(\alpha,\alpha,T)$ plotted as a function of α for (a) $\lambda_0 d_i=1$ and (b) $\lambda_0 d_i=3$ with $\kappa=0.5$. Curve a, $T/T_d=0.05$; b, $T/T_d=0.3$; c, $T/T_d=0.6$; and d, Sigrist and Rice's result (SR theory).

$$R_N J_C(\alpha,\alpha,T)=\frac{4\pi\overline{R_N}\Delta_d(0)}{3e}\,[2\sqrt{2}\,\cos\alpha-\cos(2\alpha)]. \tag{83}$$

The temperature dependence of $J_C(\alpha,\alpha,T)$ is insensitive to the change in α. For nonzero $\lambda_0 d_i$, $J_C(\alpha,\alpha,T)$ depends on α significantly. Especially for a low-conductance junction ($\sigma_N\to 0$), $J_C(\alpha,\alpha,T)$ is strongly enhanced at low temperatures due to the formation of ZES's. For $0<\varphi<\pi$ ($-\pi<\varphi<0$), $F(\theta,i\omega_n,\varphi)$ becomes positive (negative), independent of θ. The magnitude of I_1 in Eq. (66) becomes dominant for any β. Consequently, with the increase of $\lambda_0 d_i$, the φ dependence of $I(\varphi)$ becomes sinusoidal. The temperature dependence of the maximum Josephson current $J_C(\alpha,\alpha,T)$ is plotted in Fig. 11. Since the quantity $F(\theta,i\omega_n,\varphi)$ is positive, independent of θ, the maximum Josephson current $R_N J_C(\alpha,\alpha,T)$ is a monotonically increasing function with the decrease of temperatures. The enhancement of $J_C(\alpha,\alpha,T)$ with the decrease of temperature is most significant for $\alpha=\beta=\pi/4$. To understand these features, it is instrumental to perform the summation of ω_n analytically, which can be only possible for the special cases $\alpha=\beta=0$ and $\alpha=\beta=\pi/4$. For $\alpha=\beta=\pi/4$, where $\overline{\Delta}_{L(R)}(\theta_\pm)=\pm\overline{\Delta}_d(T,\theta)=\pm\overline{\Delta}_d(T)\sin(2\theta)$ is satisfied, the resulting $R_N I(\varphi)$ becomes

$$R_N I(\varphi)=\frac{\pi\overline{R_N}}{e}\int_{-\pi/2}^{\pi/2}\frac{\overline{\Delta}_d(T,\theta)\sigma_N\cos\theta\,\sin\varphi}{2\sqrt{\sigma_N}\,\cos(\varphi/2)}\times\tanh\left[\frac{\overline{\Delta}_d(T,\theta)\cos(\varphi/2)\sqrt{\sigma_N}}{2k_BT}\right]d\theta \tag{84}$$

and, for $\sqrt{\sigma_N}|\overline{\Delta}_d(T,\theta)|\ll 2k_BT$,

$$R_N J_C(\pi/4,\pi/4,T)=\frac{\pi\overline{R_N}}{4ek_BT}\int_{-\pi/2}^{\pi/2}\overline{\Delta}_d^2(T,\theta)\sigma_N d\theta. \tag{85}$$

Since the temperature is included in the denominator, the Josephson current is expected to increase as the temperature is lowered. This anomalous behavior originates from the existence of ZES's at the interfaces of both the left and right superconductors [curves c in Figs. 11(a) and 11(b)]. At sufficiently low temperatures, i.e., $k_BT\ll\sqrt{\sigma_N}|\overline{\Delta}_d(T,\theta)|$, $R_N J_C(\pi/4,\pi/4,T)$ is given as

$$R_N J_C(\pi/4,\pi/4,T)\sim\frac{\pi\overline{R_N}}{e}\int_{-\pi/2}^{\pi/2}|\overline{\Delta}_d(T,\theta)|\sqrt{\sigma_N}\,\cos\theta\,d\theta. \tag{86}$$

Since the order of the magnitude of $\overline{R_N}$ is proportional to the inverse of σ_N, $R_N J_C(\pi/4,\pi/4,T)$ at zero temperature is proportional to the inverse of $\sqrt{\sigma_N}$. Hence we can expect a large magnitude of $R_N J_C(\pi/4,\pi/4,T)$ for a low-conductance junction with $\alpha=\beta=\pi/4$. Figure 12 shows the calculated results of $B(\alpha,\alpha,T)$ as a function of α for various temperatures. Curves a–c show that $B(\alpha,\alpha,T)$ takes the maximum value at $\alpha=\pi/4$ in the low-temperature region. As the temperature is lowered and as $\lambda_0 d_i$ is increased, the magnitude of $B(\pi/4,\pi/4,T)$ is enhanced. This anomalous α dependence cannot be explained in the framework of SR theory (curve d). Since ZES's are formed at the interfaces of both left and right superconductors, the ω_n dependence of $H(i\omega_n)$ is drastically changed as compared to Eq. (81). For sufficiently low temperature with small σ_N, i.e., $\sqrt{\sigma_N}|\overline{\Delta}_d(T,\theta)|\ll\omega_n$, $H(i\omega_n)$ becomes

$$H(i\omega_n)=8\int_{\pi/4-\alpha}^{\pi/4+\alpha}\frac{\sigma_N\cos\theta|\overline{\Delta}_L(\theta_+)|^2|\overline{\Delta}_L(\theta_-)|^2}{\omega_n^2[|\overline{\Delta}_L(\theta_+)|+|\overline{\Delta}_L(\theta_-)|]^2}\,d\theta\propto\omega_n^{-2}, \tag{87}$$

with $\overline{\Delta}_L(\theta_\pm)=\overline{\Delta}_R(\theta_\pm)$, and the resulting $R_N I_C(T)$ is proportional to the inverse of T. This anomalous ω_n dependence of $H(i\omega_n)$ is the origin of the deviation from that of SR theory.

Third, we assume a mirror-type junction ($\alpha=-\beta$). Table IV shows that $F(\theta,i\omega_n,\varphi)$ becomes negative (positive) for

TABLE IV. $0 \leqslant \alpha \leqslant \pi/4$. Condition for the formation of the bound states and the sign of $F(\theta, i\omega_n, \varphi)$ with $\alpha = -\beta$ in the $d/I/d$ junction.

	Zero-energy states ($\sigma_N \to 0$) left side	Zero-energy states ($\sigma_N \to 0$) right side	Sign of $F(\theta, i\omega_n, \varphi)$ $(0 < \varphi < \pi)$	Sign of $F(\theta, i\omega_n, \varphi)$ $(-\pi < \varphi < 0)$
$\pi/4+\alpha < \theta < \pi/2$	No	No	+	−
$\pi/4-\alpha < \theta < \pi/4+\alpha$	Yes	Yes	−	+
$-\pi/4+\alpha < \theta < \pi/4-\alpha$	No	No	+	−
$-\pi/4-\alpha < \theta < -\pi/4+\alpha$	Yes	Yes	−	+
$-\pi/2 < \theta < -\pi/4-\alpha$	No	No	+	−

$\pm\pi/4-\alpha < \pi < \pm\pi/4+\alpha$ with $0 < \varphi < \pi$ $(-\pi < \varphi < 0)$. These conditions happen to coincide with those of the formation of ZES's both at the left and right interfaces. Typical $I(\varphi)$ and $R_N J_C(\alpha, -\alpha, T)$ are shown in Figs. 13 and 14, respectively. When $\lambda_0 d_i = 0$, the magnitude of $I(\varphi)$ increases with the decrease in temperatures [Fig. 13(a) and curves *a* in Fig. 14]. But when $\lambda_0 d_i$ becomes nonzero, the magnitudes of $I(\varphi)$ and $J_C(\alpha, -\alpha, T)$ show nonmonotonous behavior with temperature [Fig. 13(b) and curves *b*, and *c* in Fig. 14(a)]. As α increases, $I(\varphi)$ changes sign with decrease in T for fixed φ [Figs. 13(c) and 13(d)]. The magnitude of $J_C(\alpha, -\alpha, T)$ has an anomalous temperature dependence as shown in curves *b* and *c* in Figs. 14(b) and 14(c). In this case, $\overline{H(i\omega_n)}$ for a small magnitude of ω_n and $\sqrt{\sigma_N}|\Delta_d(T,\theta)| \ll \omega_n$ is expressed as

$$\overline{H(i\omega_n)} = -8 \int_{\pi/4-\alpha}^{\pi/4+\alpha} \frac{\sigma_N \cos\theta |\overline{\Delta_L}(\theta_+)|^2 |\overline{\Delta_L}(\theta_-)|^2}{\omega_n^2 [|\overline{\Delta_L}(\theta_+)| + |\overline{\Delta_L}(\theta_-)|]^2} \, d\theta \propto \omega_n^{-2}, \tag{88}$$

with $\overline{\Delta_L}(\theta_\pm) = \overline{\Delta_R}(\theta_\mp)$. This anomalous ω_n dependence is similar to the case of $\alpha = \beta$ and induces the nonmonotonous temperature dependences of $J_C(\alpha, -\alpha, T)$. To understand this effect clearly, three parameters $G_p(\varphi)$, $G_n(\varphi)$, and φ_M are defined. Since the sign of $R_N I(\varphi)$ has a φ dependence, $R_N I(\varphi)$ is decomposed into a negative component $G_n(\varphi)$ and a positive component $G_p(\varphi)$. When $0 < \varphi < \pi$, they are expressed as

$$G_n(\varphi) = \frac{\overline{R_N} \pi k_B T}{e} \left\{ \sum_{\omega_n} \int_{-\pi/4-\alpha}^{-\pi/4+\alpha} F(\theta, i\omega_n, \varphi) \sigma_N \cos\theta \, d\theta + \int_{\pi/4-\alpha}^{\pi/4+\alpha} F(\theta, i\omega_n, \varphi) \sigma_N \cos\theta \, d\theta \right\} \sin\varphi, \tag{89}$$

and $G_p(\varphi) = R_N I(\varphi) - G_n(\varphi)$. On the other hand, when $-\pi < \varphi < 0$, they are given by

$$G_p(\varphi) = \frac{\overline{R_N} \pi k_B T}{e} \left\{ \sum_{\omega_n} \int_{-\pi/4-\alpha}^{-\pi/4+\alpha} F(\theta, i\omega_n, \varphi) \sigma_N \cos\theta \, d\theta + \int_{\pi/4-\alpha}^{\pi/4+\alpha} F(\theta, i\omega_n, \varphi) \sigma_N \cos\theta \, d\theta \right\} \sin\varphi, \tag{90}$$

and $G_n(\varphi) = R_N I(\varphi) - G_p(\varphi)$. The quantity φ_M $(-\pi < \varphi_M < \pi)$ is defined as the phase difference giving the maximum amplitude of $I(\varphi)$. In Fig. 15, $|G_n(\varphi_M)|$ and $G_p(\varphi_M)$ are

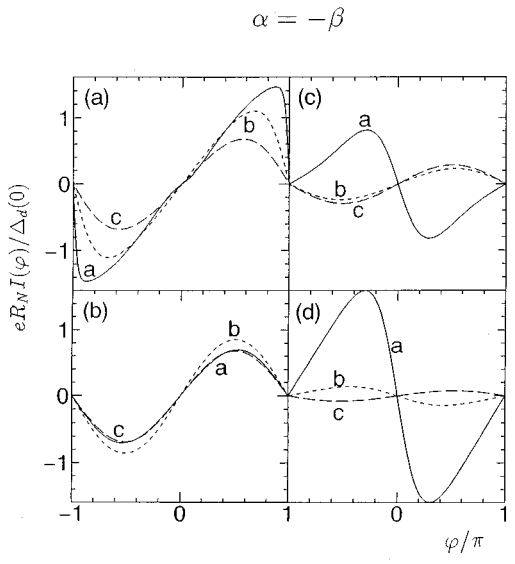

FIG. 13. Josephson current $I(\varphi)$ in $d/I/d$ junction plotted as a function of φ for $\kappa = 0.5$ and $\alpha = -\beta$: (a) $\alpha = 0.05\pi$, $\lambda_0 d_i = 0$, (b) $\alpha = 0.05\pi$, $\lambda_0 d_i = 2$, (c) $\alpha = 0.1\pi$, $\lambda_0 d_i = 2$, and (d) $\alpha = 0.12\pi$, $\lambda_0 d_i = 2$. Curve *a*, $T/T_d = 0.05$; *b*, $T/T_d = 0.3$; and *c*, $T/T_d = 0.6$.

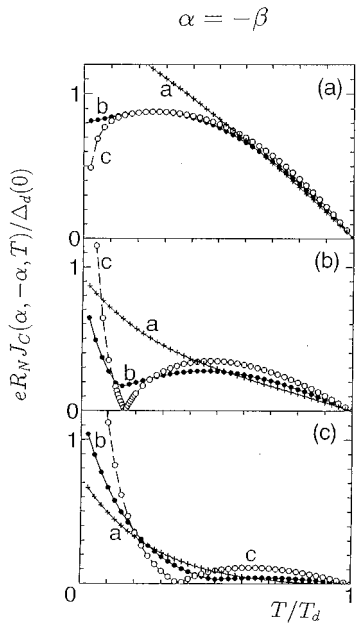

FIG. 14. Maximum Josephson current $J_C(\alpha, \beta, T)$ in $d/I/d$ junction with $\alpha = -\beta$ plotted as a function of temperature with $\kappa = 0.5$: (a) $\alpha = 0.05\pi$, (b) $\alpha = 0.1\pi$, and (c) $\alpha = 0.12\pi$. Curve *a*, $\lambda_0 d_i = 0$; *b*, $\lambda_0 d_i = 1$; and *c*, $\lambda_0 d_i = 3$.

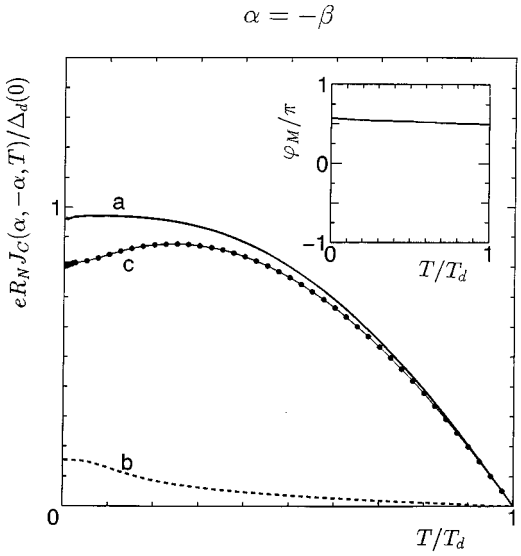

FIG. 15. Positive and negative components of $J_C(\alpha,-\alpha,T)$ obtained from curve b of Fig. 14(a) as a function of temperature: Curve a, $G_p(\varphi_M)$; b, $|G_n(\varphi_M)|$; and c, $R_N J_C(\alpha,-\alpha,T)$. In the inset φ_M is plotted as a function of temperature.

plotted using the same parameters as curve b in Fig. 14(a). In the inset of Fig. 15, the temperature dependence of φ_M is also plotted. At the low-temperature region, $G_p(\varphi_M)$ is almost constant while $|G_n(\varphi_M)|$ is enhanced reflecting the formation of ZES's. This unbalanced dependence is the origin of the suppression of $R_N J_C(\alpha,-\alpha,T)$ at low temperature. In some cases, with the increase in α, the jump of φ_M occurs as shown in Fig. 16, which is plotted using the same parameters as curve b in Fig. 14(b) (see the inset of Fig. 16). Near the temperature of the jump, $T \sim T_j$, the shape of $I(\varphi)$ changes as shown in Fig. 17. The nonmonotonous temperature dependence and the enhancement of $R_N J_C(\alpha,-\alpha,T)$ below T_j originate from the jump of φ_M from positive to negative and from the enhancement of $G_p(\varphi_M)$ with negative φ_M. With a further increase of α, φ_M stays negative, independent of temperature. In this case, $R_N J_C(\alpha,-\alpha,T)$ becomes a monotonically increasing function with the decrease of temperatures since $G_p(\varphi_M) > |G_n(\varphi_M)|$ is satisfied for all temperatures (Fig. 18). The comparison of our results with that of SR theory for a fixed temperature is plotted in Fig. 19. There is a double minimum in $B(\alpha,-\alpha,T)$. The width of the peak at $\alpha = \pi/4$ increases as the temperature is decreased. The height of the peak enhances with the increase of the magnitude of $\lambda_0 d_i$. These features are remarkably different from those expected from SR theory (curve d).

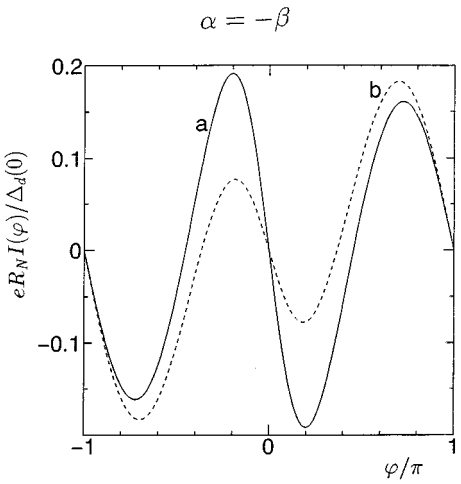

FIG. 17. Josephson current $I(\varphi)$ is plotted near T_j, where jump of the φ_M occurs: Curve a, $T = 0.125 T_d$; b, $T = 0.175 T_d$. The same parameters are used as in Fig. 16.

Finally, the applicability of AB and SR theories is summarized. Both theories assume junctions with low conduc-

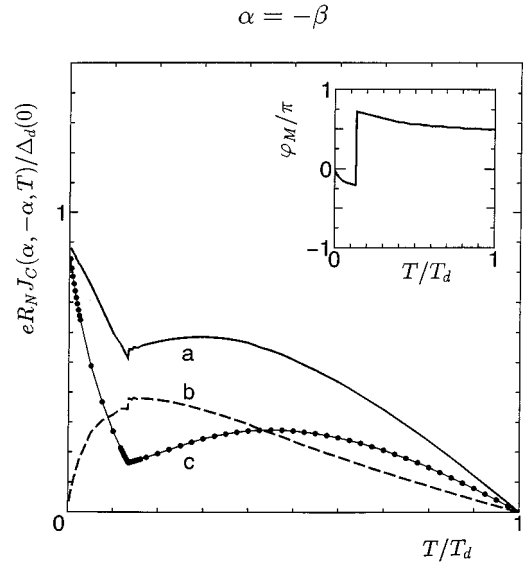

FIG. 16. Positive and negative components of $J_C(\alpha,-\alpha,T)$ obtained from curve b of Fig. 14(b) as a function of temperature: Curve a, $G_p(\varphi_M)$; b, $|G_n(\varphi_M)|$; and c, $R_N J_C(\alpha,-\alpha,T)$. In the inset φ_M is plotted as a function of temperature.

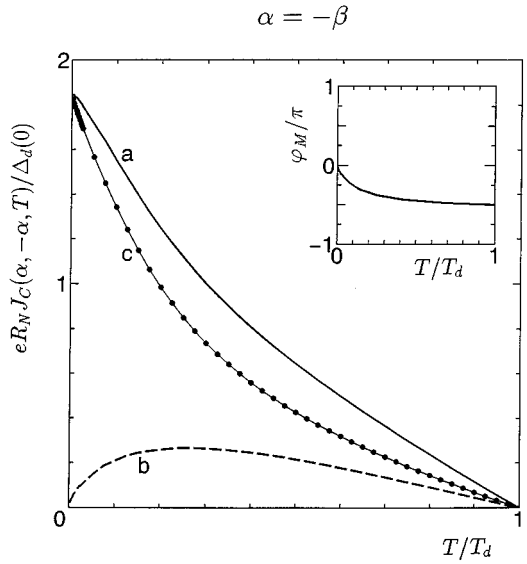

FIG. 18. Positive and negative components of $J_C(\alpha,-\alpha,T)$ obtained for $\alpha = -\beta = 0.15\pi$, $\lambda_0 d_i = 1$, and $\kappa = 0.5$: Curve a, $G_p(\varphi_M)$; b, $|G_n(\varphi_M)|$; and c, $R_N J_C(\alpha,-\alpha,T)$. In the inset φ_M is plotted as a function of temperature.

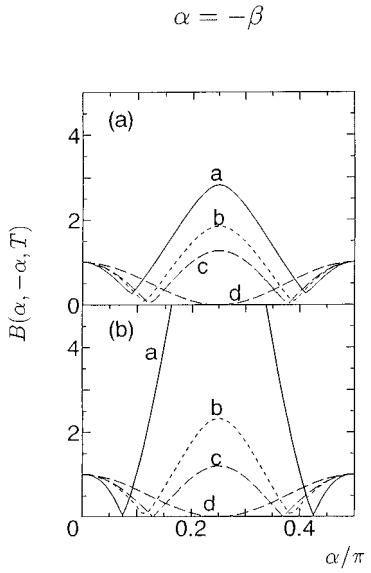

FIG. 19. $B(\alpha,-\alpha,T)$ plotted as a function of α with $\kappa=0.5$ for (a) $\lambda_0 d_i=1$ and (b) $\lambda_0 d_i=3$. Curve a, $T/T_d=0.05$; b, $T/T_d=0.3$; c, $T/T_d=0.6$; and d, Sigrist and Rice's result (SR theory).

tance and ignore the existence of the ZES's. We can apply AB theory only when there is no ZES for every θ at the interface; i.e., $\alpha=\beta=0$ is satisfied. In SR theory, only the current component which flows perpendicular to the interface is considered. In the case when one of the interfaces of the superconductor has no ZES for every θ, i.e., $\alpha=0$ ($\beta=0$) is satisfied, the $\beta(\alpha)$ dependence of the maximum Josephson current is expressed by SR theory fairly well. However, when both superconductors have ZES's, e.g., for $\alpha=\beta$ or $\alpha=-\beta$, a large deviation exists from SR theory.

V. JOSEPHSON EFFECT ALONG THE *c* AXIS

In the previous two sections, we discussed the Josephson effect in two-dimensional models. This section presents the Josephson current along the c axis which takes into account the three-dimensional effect. For the simplest model calculation, we consider an s-wave superconductor/insulator/nearly-two-dimensional $d_{x^2-y^2}$-wave superconductor ($s/I/d'$) junction [Fig. 20(a)] and a nearly-two-dimensional $d_{x^2-y^2}$-wave superconductor/insulator/nearly-two-dimensional $d_{x^2-y^2}$-wave superconductor ($d'/I/d'$) junction [Fig. 20(b)]. For the actual high-T_c superconductors like Y-Ba-Cu-O, since the tetragonal symmetry is weakly broken, the s-wave component is mixed with the $d_{x^2-y^2}$-wave components. To see the effect of this mixing, the properties of an s-wave superconductor/insulator/$s+d_{x^2-y^2}$-wave superconductor [$s/I/(s+d')$] junction are also discussed. We assume a spherical Fermi surface in the s-wave superconductor and a nearly two-dimensional Fermi surface in the d-wave superconductor, which is defined by restricting the z component of the Fermi surface to the region given by $-\delta<\sin^{-1}(k_{Fz}/k_F)<\delta$. The effective Fermi surface which is available for tunneling in the $s/I/d'$ junction is determined by the Fermi surface in the d-wave superconductor [see Fig. 20(c)]. The interface is assumed to be perpendicular to the z axis and is located at $z=0$ and $z=d_i$, where d_i is the thickness of the

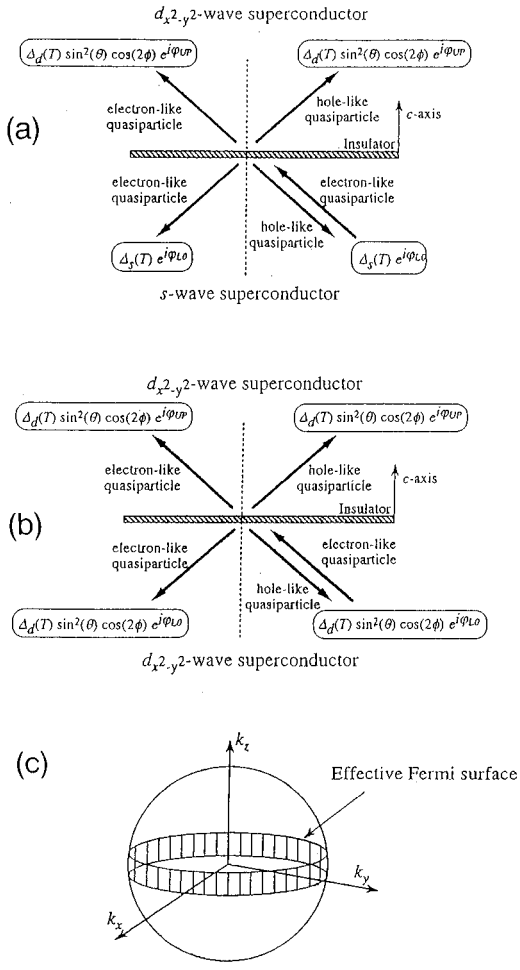

FIG. 20. Schematic illustration of the reflection and the transmission of quasiparticles at the interface of a c-axis-oriented Josephson junction: (a) s-wave superconductor/insulator/nearly-two-dimensional $d_{x^2-y^2}$-wave superconductor ($s/I/d'$) junction. (b) Nearly-two-dimensional $d_{x^2-y^2}$-wave superconductor/insulator/nearly-two-dimensional $d_{x^2-y^2}$-wave superconductor ($d'/I/d'$) junction. (c) The effective Fermi surface.

insulator. The Fermi wave numbers for x,y,z directions (k_{Fx},k_{Fy},k_{Fz}) and the effective mass m are assumed to be equal in both the lower- and upper-side superconductors. We assume that the pair potential and the Hartree potential are

$$\Delta(\mathbf{k},\mathbf{r})=\begin{cases}\overline{\Delta_{\rm lo}}(\gamma_\theta,\gamma_\phi)\exp(i\varphi_{\rm lo}), & z<0,\\ 0, & 0<z<d_i,\\ \overline{\Delta_{\rm up}}(\gamma_\theta,\gamma_\phi)\exp(i\varphi_{\rm up}), & z>d_i,\end{cases}$$

$$U(z)=\begin{cases}0, & z<0,\\ U_0, & 0<z<d_i,\\ 0, & z>d_i,\end{cases} \tag{91}$$

where γ_θ is the injection angle of the quasiparticle and γ_ϕ is the azimuthal angle in the xy (ab) plane, $\Delta(\mathbf{k},\mathbf{r})$ is the Fourier transform of $\Delta(\mathbf{s},\mathbf{r})$, $\mathbf{k}$ is the wave number, with $\exp(i\gamma_\phi)\sin\gamma_\theta\equiv k_x/|\mathbf{k}|+ik_y/|\mathbf{k}|$ and $\cos\gamma_\theta\equiv k_z/|\mathbf{k}|$ using a wave vector $\mathbf{k}$. Applying these configurations to Eq. (14), $I(\varphi)$ is obtained as

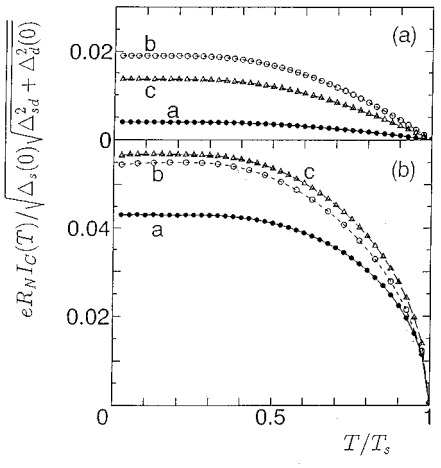

FIG. 21. Maximum Josephson current $I_C(T)$ is plotted as a function of temperature with $\kappa=0.5$ for curve a, $\lambda_0 d_i=1$, $\delta=0.1$; b, $\lambda_0 d_i=0.5$, $\delta=0.1$; and c, $\lambda_0 d_i=1$, $\delta=0.2$ (a) $s/I/d'$ junction ($\Delta_{sd}=0$) and (b) $s/I/(s+d')$ junction with $\Delta_{sd}=0.05\Delta_d(0)$.

$$I(\varphi)=\frac{e\hbar k_B T}{2im}\lim_{z'\to z}\left(\frac{\partial}{\partial z'}-\frac{\partial}{\partial z}\right)\times\sum_{\omega_n,k_x,k_y}\{\mathbf{G}(z,z',k_x,k_y,i\omega_n)\}|_{z=0}. \quad (92)$$

Here the Green's function is expressed as a function of k_x and k_y, because the translational invariance for these directions is satisfied. In general, there are four kinds of effective pair potentials for a quasiparticle with fixed γ_θ and γ_ϕ. They are $\overline{\Delta}_{\rm lo}(\gamma_{\theta,+},\gamma_\phi)$, $\overline{\Delta}_{\rm lo}(\gamma_{\theta,-},\gamma_\phi)$, $\overline{\Delta}_{\rm up}(\gamma_{\theta,+},\gamma_\phi)$, and $\overline{\Delta}_{\rm up}(\gamma_{\theta,-},\gamma_\phi)$. We assume $\overline{\Delta}_{\rm lo}(\gamma_{\theta,+},\gamma_\phi)=\overline{\Delta}_{\rm lo}(\gamma_{\theta,-},\gamma_\phi)$ and $\overline{\Delta}_{\rm up}(\gamma_{\theta,+},\gamma_\phi)=\overline{\Delta}_{\rm up}(\gamma_{\theta,-},\gamma_\phi)$ for simplicity. By inserting these pair potentials into Eq. (14) and following the described method in Sec. II, the Josephson current $I(\varphi)$ is obtained:

$$R_N I(\varphi)=\frac{\overline{R_N}k_B T}{2e}\left\{\sum_{\omega_n}\int_{\pi/2-\delta}^{\pi/2}\sin\theta\cos\theta\times d\theta\int_0^{2\pi}d\phi\,\frac{|\overline{\Delta}_{\rm lo}(\theta,\phi)|}{\Omega_{n,\rm lo}}[a_1(\theta,\phi,i\omega_n,\varphi)-\tilde{a}_1(\theta,\phi,i\omega_n,\varphi)]\right\}, \quad (93)$$

with

$$\Omega_{n,\rm lo}=\mathrm{sgn}(\omega_n)\sqrt{\Delta_{\rm lo}^2(\theta,\phi)+\omega_n^2},\quad \varphi=\varphi_{\rm lo}-\varphi_{\rm up}. \quad (94)$$

The quantity R_N denotes the normal resistance, and $\overline{R_N}$ is expressed as

$$\overline{R_N}^{-1}=\int_{\pi/2-\delta}^{\pi/2}\sigma_N\sin\theta\cos\theta\,d\theta, \quad (95)$$

where the quantity σ_N is defined in Eq. (47). The quantities $a_1(\theta,\phi,i\omega_n,\varphi)$ and $\tilde{a}_1(\theta,\phi,i\omega_n,\varphi)$ are the coefficients of Andreev reflection as discussed in Sec. II. In the following, we will restrict our discussion to the case where the time-reversal symmetry is conserved. In such a situation, J_n ($n\geqslant 1$) in Eq. (66) vanishes and $I(\varphi)=-I(-\varphi)$ is satisfied.

The resulting $R_N I(\varphi)$ is expressed as

$$R_N I(\varphi)=\frac{\overline{R_N}k_B T}{2e}\left\{\sum_{\omega_n}\int_{\pi/2-\delta}^{\pi/2}\sigma_N\cos\theta\sin\theta\,d\theta\int_0^{2\pi}F(\theta,\phi,i\omega_n,\varphi)\sin\varphi\,d\phi\right\}, \quad (96)$$

$$F(\theta,\phi,i\omega_n,\varphi)=\frac{2\overline{\Delta}_{\rm lo}(\theta,\phi)\overline{\Delta}_{\rm up}(\theta,\phi)}{(2-\sigma_N)\Omega_{n,\rm lo}\Omega_{n,\rm up}+\sigma_N[\omega_n^2+\overline{\Delta}_{\rm lo}(\theta,\phi)\overline{\Delta}_{\rm up}(\theta,\phi)\cos\varphi]}=\frac{2\overline{\Delta}_{\rm lo}(\theta,\phi)\overline{\Delta}_{\rm up}(\theta,\phi)}{[(2-\sigma_N)\Omega_{n,\rm lo}\Omega_{n,\rm up}+\sigma_N\omega_n^2]}\times\sum_{m=0}^{\infty}\left[-\frac{\sigma_N\overline{\Delta}_{\rm lo}(\theta,\phi)\overline{\Delta}_{\rm up}(\theta,\phi)\cos\varphi}{(2-\sigma_N)\Omega_{n,\rm lo}\Omega_{n,\rm up}+\sigma_N\omega_n^2}\right]^m, \quad (97)$$

with $\Omega_{n,\rm up}=\mathrm{sgn}(\omega_n)\sqrt{\Delta_{\rm up}^2(\theta,\phi)+\omega_n^2}$.

First, the Josephson current in the $s/I/d'$ junction is discussed. The pair potential felt by the quasiparticles for fixed θ and ϕ is shown in Fig. 20(a). The effective pair potentials are given as $\overline{\Delta}_{\rm lo}(\theta,\phi)=\Delta_s(T)$ and $\overline{\Delta}_{\rm up}(\theta,\phi)=\Delta_d(T)\sin^2\theta\cos(2\phi)$. By substituting these pair potentials into Eq. (97), we obtain $I(\varphi)$. Due to the ϕ integral, the terms proportional to $\cos^{2m}\varphi$ vanish, and then I_1 in Eq. (66) also vanishes. For small transparent junctions, $I(\varphi)$ becomes almost proportional to $\sin(2\varphi)$. In the case of the $[s/I/(s+d')]$ junction, the pair potential in the upper superconductor, $\overline{\Delta}_{\rm up}(\theta,\phi)$, is given as $\Delta_d(T)\sin^2\theta\cos(2\phi)+\Delta_{sd}$. $I(\varphi)$ is calculated by substituting these pair potentials into those in Eq. (97). Hereafter, we assume that both $\Delta_s(T)$ and $\Delta_d(T)$ obey the BCS relation as in Secs. III and IV. The ratios of $\Delta_s(0)/\Delta_d(0)$ and T_s/T_d are chosen to be 1/15 and 1/11. Figure 21(a) shows the temperature dependence of the maximum Josephson current of the $s/I/d$ junction for various $\lambda_0 d_i$ and δ. When $T\sim T_s$, $R_N I_C(T)$ is proportional to (T_s-T). This feature is quite different from that of AB theory. With the increase of $\lambda_0 d_i$ and with the decrease of δ, $I_C(T)$ is drastically suppressed. In the case of the $[s/I/(s+d')]$ junction, near $T\sim T_s$, $R_N I_C(T)$ is proportional to $\sqrt{T_s-T}$ as shown in Fig. 21(b) since $R_N I(\varphi)$ is proportional to $\sin(\varphi)$. The maximum Josephson current $I_C(T)$ is insensi-

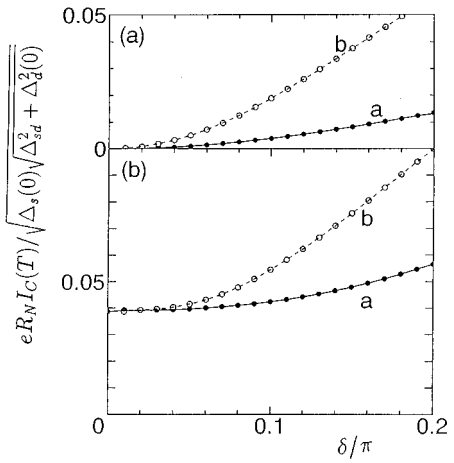

FIG. 22. Maximum Josephson current $I_C(T)$ is plotted as a function of δ at $T/T_s=0.025$ with $\kappa=0.5$ for curve a, $\lambda_0 d_i=1$; b, $\lambda_0 d_i=0.5$. (a) $s/I/d'$ junction ($\Delta_{sd}=0$) and (b) $s/I/(s+d')$ junction with $\Delta_{sd}=0.05\Delta_d(0)$.

tive to the change of $\lambda_0 d_i$ and to δ as compared to that of Fig. 21(a). To check the effect of dimensionality, the δ dependence of $R_N I(\varphi)$ is discussed. Figure 22 shows the calculated results of the δ dependence of $I_C(T)$. In the case of the $s/I/d'$ junction, $R_N I_C(T)$ decreases monotonically with the decrease of δ and finally vanishes at $\delta=0$ [Fig. 22(a)]. This feature is independent of $\lambda_0 d_i$ and κ, while in the case of the $s/I/(s+d')$ junction $R_N I_C(T)$ stays nonzero at $\delta=0$ [Fig. 22(b)]. In fact, we can analytically calculate $R_N I_C(T)$ at the two-dimensional limit, i.e., $\delta\rightarrow 0$, where

$$R_N I(\varphi)=R_N I_C(T)\sin\varphi \tag{98}$$

is satisfied. Using the fact that the $\sigma_N \cos\theta$ is expressed as

$$\lim_{\delta\rightarrow 0}\sigma_N\cos\theta|_{\theta=\pi/2-\delta}\sim\delta^3, \tag{99}$$

$R_N I_C(T)$ of the $s/I/d'$ junction is transformed into

$$R_N I_C(T)=\frac{k_B T}{2e}\sum_n \int_0^{2\pi} d\phi \times\frac{\overline{\Delta}_{\rm lo}(\pi/2,\phi)\overline{\Delta}_{\rm up}(\pi/2,\phi)}{\sqrt{\omega_n^2+\overline{\Delta}_{\rm lo}^2(\pi/2,\phi)}\sqrt{\omega_n^2+\overline{\Delta}_{\rm up}^2(\pi/2,\phi)}}. \tag{100}$$

Due to the ϕ integral, $R_N I_C(T)$ completely vanishes, independent of $\lambda_0 d_i$ and κ. On the other hand, in the case of the $d'/I/(s+d')$ junction, $R_N I_C(T)$ is given as

$$R_N I_C(T)=\frac{k_B T}{2e}\sum_n \int_0^{2\pi} d\phi \times\frac{\Delta_s(T)\Delta_{sd}}{\sqrt{\omega_n^2+\Delta_s^2(T)}\sqrt{\omega_n^2+[\Delta_d(T)\cos 2\phi+\Delta_{sd}]^2}}. \tag{101}$$

It takes a nonzero value even at the two-dimensional limit.

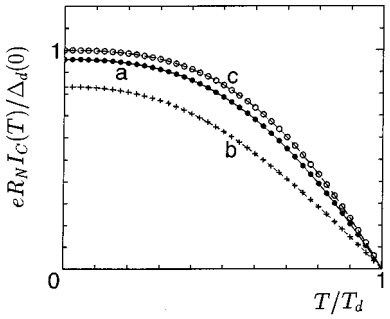

FIG. 23. Maximum Josephson current $I_C(T)$ for $d'/I/d'$ junction is plotted as a function of temperatures for $\kappa=0.5$: Curve a, $\lambda_0 d_i=1$, $\delta=0.1$; b, $\lambda_0 d_i=1$, $\delta=0.2$; and c, two-dimensional limit, i.e., $\delta=0$.

Next, the properties of the $d'/I/d'$ junction[84,85] are discussed. In this case, both $\overline{\Delta}_{\rm up}(\theta,\phi)$ and $\overline{\Delta}_{\rm lo}(\theta,\phi)$ are given by $\Delta_d(T)\cos(2\phi)\sin^2\theta$. Taking the summation of the Matsubara frequency in Eq. (97) analytically, $R_N I(\varphi)$ is expressed as

$$R_N I(\varphi)=\frac{\pi\overline{R_N}}{e}\int_{\pi/2-\delta}^{\pi/2} d\theta \times\int_0^{2\pi} G(T,\theta,\phi,\varphi)\sigma_N\cos\theta\sin\theta\,\sin\varphi\; d\phi, \tag{102}$$

with

$$G(T,\theta,\phi,\varphi)=\frac{\Delta_d(T)\sin^2\theta\,\cos(2\phi)}{2\sqrt{1-\sigma_N\sin^2(\varphi/2)}} \times\tanh\left[\frac{\Delta_d(T)\sin^2\theta\,\cos(2\phi)\sqrt{1-\sigma_N\sin^2(\varphi/2)}}{2k_B T}\right]. \tag{103}$$

The maximum Josephson current $R_N I_C(T)$ is always a monotonically increasing function with the decrease of temperatures as shown in Fig. 23. This feature shows a remarkable difference from that of the $d/I/d$ junction discussed in the preceding section. In the two-dimensional limit ($\delta\rightarrow 0$), $R_N I(\varphi)$ is simplified as

$$R_N I(\varphi)=\left\{\int_0^{2\pi}\frac{\Delta_d(T)\cos(2\phi)}{4e} \times\tanh\left[\frac{\Delta_d(T)\cos(2\phi)}{2k_B T}\right]d\phi\right\}\sin\varphi. \tag{104}$$

In this limit, $R_N I(\varphi)$ is independent of λ_0 and κ. Furthermore, at zero temperature, $R_N I_C(T)e/\Delta_d(0)$ becomes exactly 1. The corresponding quantity in the $s/I/s$ junction obtained by AB theory is $\pi/2$. The difference directly reflects the distribution of the pair potential amplitude in momentum space.

VI. SUMMARY AND DISCUSSION

An analytical formula for the dc Josephson current in spin-singlet anisotropic superconductors has been presented. We have taken into account the fact that quasiparticles ''feel'' the different signs of the pair potentials depending on the directions of their motions.[42–46] Our formula is general in the sense that several existing formulas for the Josephson current can be derived as limiting cases.[11,26,66,69,78,79,82] This formula is valid, even when the time-reversal symmetry is broken: i.e., the pair potential of the superconductor becomes a complex number. Since the multiple Andreev reflection and the normal reflection at the interface are completely included, the formula can be applicable for arbitrary barrier height case.

Applying our formula, the Josephson current is calculated for various junction geometries. The calculated results show several anomalous behaviors which are not expected for Josephson junctions of conventional s-wave superconductors. Especially, three important features are predicted for Josephson junctions including d-wave superconductors.

(1) For a fixed phase difference between two superconductors, the component of the Josephson current becomes either positive or negative depending on the injection angle of the quasiparticle.

(2) In some situations, the phase difference φ_0, which gives the free energy minima, is located at neither zero nor π.

(3) When the crystal axis is tilted from the interface normal, zero-energy states (ZES's), i.e., midgap states, are formed near the interface depending on the angle of the crystal axis and the injection angle of the quasiparticle. The existence of ZES's enhances the Josephson current at low temperatures.

These features will be confirmed if they are actually measured in experiments.

Many experimental trials have already been performed on Josephson junctions made of high-T_c superconductors. Sun *et al.*[86] and Katz *et al.*[87] observed the Josephson current in c-axis-oriented Pb/YBCO junctions. The observed $R_N I_C(T)$ is proportional to $\sqrt{T_s - T}$ near T_s, where T_s is the transition temperature of Pb. On the other hand, Dursoy *et al.*[88] tried similar experiments on Bi-Sr-Ca-Cu-O (BSCCO)/Pb, and they did not observe the Josephson current. We believe that these results do not contradict each other.[76] In the case of YBCO, the presence of orthorhombic distortion induces the mixing of s-wave components in the d-wave pair potential.[76] If we assume $\Delta_s(0) = 1.2$ meV, $\Delta_d(0) = 18$ meV, and $\Delta_{sd} = 0.09$ meV, the obtained $R_N I_C(T)$ is about 0.2–0.3 mV at zero temperature and proportional to $\sqrt{T_s - T}$ near T_s. These features are qualitatively consistent with experimental results of YBCO/Pb. While in the case of BSCCO/Pb, since the crystal structure of BSCCO is tetragonal, the mixing of the s-wave components is not expected. The leading term of $I(\varphi)$ should be the $\sin(2\varphi)$ component whose amplitude is far less than that of the $\sin(\varphi)$ component of $I(\varphi)$ in ordinary junctions. Furthermore, since BSCCO is more like a two-dimensional material as compared to YBCO, the Josephson current was enormously reduced as was shown in Fig. 22(a). For these reasons, it is very difficult to observe the Josephson current in experiments using BSCCO/Pb. Recently, Kleiner *et al.* tried to observe the $\sin(2\varphi)$ dependence of the Josephson current from microwave-induced steps.[89] However, the existence of this term was not confirmed in their experiments. This may be due to the two-dimensional Fermi surface of YBCO and the low transparency of the junction.

The most fascinating experiment is to observe the nonmonotonous temperature dependence of the Josephson current which is predicted in this paper especially for mirror-type grain junctions. This feature is expected only when ZES's are formed at the interface of both left and right superconductors and the sign change of the Josephson current occurs as a function of injection angle. As far as we know, such results have not been reported yet, and we believe it will be observed in the future.

Throughout this paper, the spatial dependence of the pair potentials is assumed to be constant. Even if the depletion of the pair potentials around the interface is taken into account, the ZES's does not vanish at all[53,54,56,57,90] and the essential results will not be changed. After our work,[63,64] Barash, Burkhardt, and Rainer calculated the Josephson current in the grain boundary $d/I/d$ junction based on a quasiclassical method which is different from our formulation.[91,92] Their theory includes the effect of roughness and the self-consistency of the spatial dependence of the pair potential. Since the analytical formula of the Josephson current corresponding to Eqs. (58) and (64) is not explicitly presented in their papers,[91,92] a direct comparison between the two theories cannot be made at present. However, the qualitative features of the Josephson current, i.e., a nonmonotonous temperature dependence of the Josephson current and anomalous phase dependence, are not changed at all when the effect of the roughness is small. The relation between their results and ours will be clarified in the near future. In this paper, only the Josephson current with zero voltage is discussed. Very recently, Barash and Svidzinsky[93] investigated the singular behavior of the quasiparticle current[94] and the Josephson current for nonzero voltage in a $d/I/d$ junction in the limit of a low-transparency coefficient. To clarify the Josephson current and the quasiparticle current for arbitrary transparency is also a challenging future problem.

ACKNOWLEDGMENTS

We would like to express our sincerest gratitude to K. Kajimura, M. Koyanagi, and A. Bacala for a critical reading of our paper. We would also thank Yu. S. Barash, H. Burkhardt, A. van Otterlo, K. Nagai, K. Kuboki, H. Kawamura, S. Yip, J. A. Sauls, K. Ueda, and S. Maekawa for valuable discussions and encouragement of our works. One of the authors (Y.T.) is supported by a Grant-in-Aid for Scientific Research in Priority Areas, ''Anomalous metallic state near the Mott transition.'' The computational aspect of this work has been done using the facilities of the Supercomputer Center, Institute for Solid State Physics, University of Tokyo, and the Computer Center, Institute for Molecular Science, Okazaki National Research Institutes.

[1] Z.-X. Shen, D. S. Dessau, B. O. Well, D. M. King, W. E. Spicer, A. J. Arko, D. Marshall, L. W. Lombardo, A. Kapitulnik, P. Dicknison, S. Doniach, J. DiCarlo, A. G. Loeser, and C. H. Park, Phys. Rev. Lett. **70**, 1553 (1993).
[2] W. N. Hardy, D. A. Bonn, D. C. Morgan, R. Liang, and K. Zhang, Phys. Rev. Lett. **70**, 3999 (1993).
[3] N. E. Bickers, D. J. Scalapino, and S. R. White, Phys. Rev. Lett. **62**, 961 (1989).
[4] P. Monthoux, A. V. Balatsky, and D. Pines, Phys. Rev. B **47**, 6069 (1993).
[5] T. Moriya, Y. Takahashi, and K. Ueda, Physica C **185**, 114 (1991).
[6] Y. Suzumura, Y. Hasegawa, and H. Fukuyama, J. Phys. Soc. Jpn. **57**, 2768 (1988).
[7] E. Dagotto and J. Riera, Phys. Rev. Lett. **70**, 682 (1992).
[8] V. B. Geshkenbein, A. I. Larkin, and A. Barone, Phys. Rev. B **36**, 235 (1987).
[9] S. Yip, O. F. de Alcantara Bonfim, and P. Kumar, Phys. Rev. B **41**, 11 214 (1990).
[10] L. N. Bulaevskii, V. V. Kuzii, and A. A. Sobyanin, JETP Lett. **25**, 290 (1977).
[11] M. Sigrist and T. M. Rice, J. Phys. Soc. Jpn. **61**, 4283 (1992); J. Low Temp. Phys. **95**, 389 (1994); Rev. Mod. Phys. **67**, 503 (1995).
[12] D. A. Wollman, D. J. van Harlingen, W. C. Lee, D. M. Ginsberg, and A. J. Leggett, Phys. Rev. Lett. **71**, 2134 (1993).
[13] D. J. Van Harlingen, Rev. Mod. Phys. **67**, 515 (1995).
[14] C. C. Tsuei, J. R. Kirtley, C. C. Chi, L. S. Yu-Jahnes, A. Gupta, T. Shaw, J. Z. Sun, and M. B. Ketchen, Phys. Rev. Lett. **73**, 593 (1994).
[15] A. Mathai, Y. Gim, R. C. Black, A. Amar, and F. C. Wellstood, Phys. Rev. Lett. **74**, 4523 (1995).
[16] I. Iguchi and Z. Wen, Phys. Rev. B **49**, 12 388 (1994).
[17] J. R. Kirtley, C. C. Tsuei, M. Rupp, J. Z. Sun, Lock See Yu-Jahnes, A. Gupta, and M. B. Ketchen, Phys. Rev. Lett. **76**, 1336 (1996).
[18] D. A. Brawner and H. R. Ott, Phys. Rev. B **50**, 6530 (1994).
[19] A. Millis, Phys. Rev. B **49**, 15 408 (1994).
[20] A. Barone, Nuovo Cimento D **16**, 1635 (1994).
[21] A. F. Andreev Zh. Eksp. Teor. Fiz. **46**, 1823 (1964) [Sov. Phys. JETP **19**, 1228 (1964)].
[22] Y. Tanaka, Phys. Rev. Lett. **72**, 3871 (1994), Physica C **235–240**, 3205 (1994).
[23] S. Yip, J. Low Temp. Phys. **91**, 203 (1993).
[24] Yu. S. Barash, A. V. Galaktionov, and A. D. Zaikin, Phys. Rev. B **52**, 665 (1995).
[25] Yu. S. Barash, A. V. Galaktionov, and A. D. Zaikin, Phys. Rev. Lett. **75**, 1676 (1995).
[26] S. Yip, Phys. Rev. B **52**, 3087 (1995).
[27] C. Bruder, A. van Otterlo, and G. T. Zimanyi, Phys. Rev. B **51**, 12 904 (1994).
[28] A. B. Kuklov, Phys. Rev. B **52**, 6729 (1995).
[29] Weiyi Zhang, Phys. Rev. B **52**, 3772 (1995); **52**, 12 538 (1995).
[30] G. Deutscher and R. Maynard, Europhys. Lett. **30**, 361 (1995).
[31] C. R. Hu, Phys. Rev. Lett. **72**, 1526 (1994).
[32] J. Geerk, X. X. Xi, and G. Linker, Z. Phys. B **73**, 329 (1988).
[33] T. Walsh, Int. J. Mod. Phys. A **6**, 125 (1992).
[34] I. Iguchi, Physica C **185–189**, 241 (1991).
[35] S. Kashiwaya, M. Koyanagi, M. Matsuda, and K. Kajimura, Physica B **194–196**, 2119 (1994).
[36] L. Alff, H. Takashima, S. Kashiwaya, N. Terada, T. Ito, K. Oka, M. Koyanagi, and Y. Tanaka (unpublished).
[37] S. Tanaka, E. Ueda, M. Sato, K. Tamasaku, and S. Uchida, J. Phys. Soc. Jpn. **64**, 1476 (1995); **65**, 2212 (1996).
[38] M. Covington, F. Xu, C. A. Mirkin, W. L. Feldmann, and L. H. Greene, Czech. J. Phys. **46**, 1341 (1996).
[39] P. Richter, A. Beck, O. M. Froehlich, R. Gross, and G. Koren, Czech. J. Phys. **46**, 1303 (1996).
[40] M. Suzuki, M. Taira, and X. Zheng, Czech. J. Phys. **46**, 1351 (1996).
[41] Y. Tanaka and S. Kashiwaya, Phys. Rev. B **53**, 9371 (1996).
[42] S. Kashiwaya, Y. Tanaka, H. Takashima, Y. Koyanagi, and K. Kajimura, Phys. Rev. B **51**, 1350 (1995).
[43] Y. Tanaka and S. Kashiwaya, Phys. Rev. Lett. **74**, 3451 (1995).
[44] A. Millis, D. Rainer, and J. A. Sauls, Phys. Rev. B **38**, 4504 (1988).
[45] C. Bruder, Phys. Rev. B **41**, 4017 (1990).
[46] J. Kurkijärvi and D. Rainer, in *Modern Problems in Condensed Matter Sciences*, edited by W. P. Halperin and L. P. Pitaevskii (Elsevier, Amsterdam, 1989).
[47] J. F. Zasadzinski, N. Tralshawala, P. Romeno, Q. Huang, Jun Chen, and K. E. Gray, J. Phys. Chem. Solids **53**, 1635 (1992).
[48] M. Oda, C. Manabe, and M. Ido, Phys. Rev. B **53**, 2253 (1996).
[49] Ch. Renner and O. Fisher, Phys. Rev. B **51**, 9208 (1995).
[50] M. Nantoh, T. Hasegawa, W. Yamaguchi, K. Kitazawa, M. Kawasaki, K. Fujito, and H. Koinuma, Physica C **242**, 277 (1995).
[51] K. Kitazawa, Science **271**, 313 (1996).
[52] S. Kashiwaya, Y. Tanaka, M. Koyanagi, and K. Kajimura, in *Advances in Superconductivity VII*, edited by K. Yamafuji and T. Morishita (Springer-Verlag, Tokyo, 1995), p. 45; Jpn. J. Appl. Phys. **34**, 4555 (1995); J. Phys. Chem. Solids **56**, 1721 (1995); Phys. Rev. B **53**, 2667 (1996).
[53] Y. Nagato and K. Nagai, Phys. Rev. B **51**, 16 254 (1995).
[54] K. Yamada, Y. Nagato, S. Higashitani, and K. Nagai, J. Phys. Soc. Jpn. **65**, 1540 (1996).
[55] Jian Yang and C. R. Hu, Phys. Rev. B **50**, 16 766 (1994).
[56] M. Matsumoto and H. Shiba, J. Phys. Soc. Jpn. **64**, 1703 (1995); **64**, 3384 (1995); **64**, 4867 (1995); **65**, 2194 (1996).
[57] L. J. Buchholtz, M. Palumbo, D. Rainer, and J. A. Sauls, J. Low Temp. Phys. **101**, 1079 (1995); **101**, 1097 (1995).
[58] M. Alber, B. Bauml, R. Ernst, D. Kienle, A. Kopf, and M. Rouchal, Phys. Rev. B **53**, 5863 (1996).
[59] Y. Ohhashi, J. Phys. Soc. Jpn. **65**, 823 (1996).
[60] P. M. A. Cook, R. Raimondi, and C. J. Lambert, Phys. Rev. B **54**, 9491 (1996).
[61] J-X Zhu, Z. D. Wang, and H. X. Tang, Phys. Rev. B **54**, 7354 (1996); **54**, 12 509 (1996).
[62] J. H. Xu, J. H. Miller, and C. S. Ting, Phys. Rev. B **53**, 3604 (1996).
[63] Y. Tanaka and S. Kashiwaya, J. Phys. Chem. Solids **56**, 1761 (1995); in *Advances in Superconductivity VIII*, edited by H. Hayakawa and Y. Enomoto (Springer-Verlag, Tokyo, 1995), p. 259.
[64] Y. Tanaka and S. Kashiwaya, Phys. Rev. B **53**, R11 957 (1996).
[65] Y. Tanaka, S. Kashiwaya, M. Koyanagi, and K. Kajimura, Physica C **262**, 238 (1996).
[66] I. O. Kulik and A. N. Ome'lyanchuk, Fiz. Nizk. Temp. **4**, 296 (1978) [Sov. J. Low Temp. Phys. **4**, 142 (1978)].
[67] I. O. Kulik, Zh. Eksp. Teor. Fiz Pis'ma Red. **21**, 216 (1975) [Sov. Phys. Jetp **30**, 944 (1970)].
[68] J. Bardeen and J. L. Johnson, Phys. Rev. B **5**, 72 (1972).
[69] C. Ishii, Prog. Theor. Phys. **44**, 1525 (1970); **47**, 1464 (1972).

[70] C. W. J. Beenakker and H. van Houten, in *Nanostructures and Mesoscopic Systems*, edited by W. P. Kirk and M. A. Read (Academic, New York, 1992), p. 481.
[71] Y. Tanaka and M. Tsukada, Phys. Rev. B **44**, 7578 (1991).
[72] M. Hurd and G. Wendin, Phys. Rev. B **51**, 3754 (1995).
[73] K. Kuboki and M. Sigrist, J. Phys. Soc. Jpn. **65**, 361 (1995).
[74] T. Koyama and M. Tachiki, Phys. Rev. B **53**, 2662 (1996).
[75] M. Sigrist, D. B. Bailey, and R. B. Laughlin, Phys. Rev. Lett. **74**, 3249 (1995).
[76] M. Sigrist, K. Kuboki, P. A. Lee, A. J. Millis, and T. M. Rice, Phys. Rev. B **53**, 2835 (1996).
[77] M. B. Walker and J. Luetmmer-Strathmann, Phys. Rev. B **54**, 588 (1996).
[78] A. Furusaki and M. Tsukada, Solid State Commun. **78**, 299 (1991).
[79] G. B. Arnold, J. Low Temp. Phys. **59**, 143 (1985).
[80] G. E. Blonder, M. Tinkham, and T. M. Klapwijk, Phys. Rev. B **25**, 4515 (1982).
[81] W. L. McMillan, Phys. Rev. **175**, B559 (1967).
[82] V. Ambegaokar and A. Baratoff, Phys. Rev. Lett. **10**, 486 (1963).
[83] A. Barone and G. Paterno, *Physics and Applications of the Josephson Effect* (Wiley, New York, 1982).
[84] K. Tanabe, Y. Hidaka, S. Karimoto, and M. Suzuki, Phys. Rev. B **53**, 9348 (1996).
[85] R. Kleiner and P. Müller, Phys. Rev. B **49**, 1327 (1994).
[86] A. G. Sun, D. A. Gajewski, M. B. Maple, and R. C. Dynes, Phys. Rev. Lett. **72**, 2267 (1994).
[87] A. S. Katz, A. G. Sun, R. C. Dynes, and K. Char, Appl. Phys. Lett. **66**, 105 (1995).
[88] H. Z. Durusoy, L. R. Tagirov, and M. R. Beasley, Solid State Commun. **97**, 297 (1996).
[89] R. Kleiner, A. S. Katz, A. G. Sun, R. Summer, D. A. Gajewski, S. H. Han, S. I. Woods, E. Dantsker, B. Chen, K. Char M. B. Maple, R. C. Dynes, and J. Clarke, Phys. Rev. Lett. **76**, 2161 (1996).
[90] S. Kashiwaya, Y. Tanaka, M. Koyanagi, and K. Kajimura (unpublished).
[91] Yu. S. Barash, H. Burkhardt, and D. Rainer, Phys. Rev. Lett. **77**, 4070 (1996).
[92] H. Burkhardt (unpublished).
[93] Y. S. Barash and A. A. Svidzinsky, JETP (to be published).
[94] S. Kashiwaya, Y. Tanaka, M. Koyanagi, S. Ueno, and K. Kajimura, Physica C (to be published).